UPR^{ER}–immunity axis acts as physiological food evaluation system that promotes aversion behavior in sensing low-quality food

Pengfei Liu, Xinyi Liu, Bin Qi[1,2]

Center for Life Sciences, School of Life Sciences, Yunnan Key Laboratory of Cell Metabolism and Diseases, State Key Laboratory of Conservation and Utilization of Bio-resources in Yunnan, Yunnan University, Southwest United Graduate School, Kunming, China

Footnotes: 1 Corresponding Author (Bin Qi, Email: qb@ynu.edu.cn)

Footnotes: 2 Lead Contact (Bin Qi, Email: qb@ynu.edu.cn)

Summary

To survive in challenging environments, animals must develop a system to assess food quality and adjust their feeding behavior accordingly. However, the mechanisms that regulate this chronic physiological food evaluation system, which monitors specific nutrients from ingested food and influences food-response behavior, are still not fully understood. Here, we established a low-quality food evaluation assay system and found that heat-killed *E. coli* (HK-*E. coli),* a low sugar food, triggers cellular UPR^{ER} and immune response. This encourages animals to avoid low-quality food. The physiological system for evaluating low-quality food depends on the UPR^{ER} (IRE-1/XBP-1) - Innate immunity (PMK-1/p38 MAPK) axis, particularly its neuronal function, which subsequently regulates feeding behaviors. Moreover, animals can adapt to a low-quality food environment through sugar supplementation, which inhibits the UPR^{ER}-PMK-1 regulated stress response by increasing vitamin C biosynthesis.

This study reveals the role of the cellular stress response pathway as physiological food evaluation system for assessing nutritional deficiencies in food, thereby enhancing survival in nature environments.

Keywords: aversion behavior; UPR^{ER}; immune response; XBP-1; PMK-1; Food quality evaluation; Food sensing; *C. elegans*;

Introduction

Food is essential for the survival, growth and fitness of all animals. To adapt to fluctuating environments with a wide range of food sources, animals have developed a food evaluation system. This system enables them to identify nutrient-rich food and avoids low-quality or toxic food, thereby maximizing their survival prospects [1-3]. Various sensory neuron evaluation systems in animals has evolved to evaluate food quality through vision [4,5], olfactory [3,6-12] and gustatory senses [13-15]. Besides these sensory systems that facilitate quick feeding decisions, animals may also initiate cellular stress response programs to detect nutrition/toxin and trigger food response behaviors [16,17]. This could be one of physiological food quality evaluation systems that monitor the nutritional status of consumed food. However, the signaling events in cellular stress responses involved in evaluating of specific nutrients and the mechanisms that connect these signaling activities to food behaviors are largely unexplored. More specifically, while cellular stress response through UPR^{ER} [18] and PMK-1/p38 MAPK [19] dependent immunity in response to pathogens have been extensively studied, the functions of these cellular stress response in sensing and evaluating specific nutrients from food remain unclear.

Vitamin C is an essential micronutrient that cannot be synthesized by humans due to the loss of a key enzyme in the biosynthetic pathway [20]. Animals obtain Vitamin C from their diet and possibly also from gut microbes [21]. Vitamin C is an important physiological antioxidant and a cofactor for a family of biosynthetic

and gene regulatory monooxygenase and dioxygenase enzymes. It is also required for the biosynthesis of collagen, L-carnitine, and certain neurotransmitters [22,23]. Vitamin C has been associated with various human diseases including scurvy, immune defect and cardiovascular disease [20]. Therefore, food evaluation systems in animals for sensing Vitamin C could be critical for their fitness in nature. However, the role of the cellular stress response pathway as food evaluation system for sensing and evaluating Vitamin C remains unexplored.

In this study, using the low-quality food evaluation assay system we established [24], we uncovered the mechanism of cellular stress responses pathway as physiological food evaluation system in evaluating D-Glucose deficiency in food and downstream Vitamin C content in animals through the UPR^{ER} (IRE-1/XBP-1) - Innate immunity (PMK-1 p38 MAPK) axis. This mechanism promotes animals to leave low-quality food and is critical for their survival in nature environments.

Results

Low-quality food induces stress response in animals

Our previous studies have shown that Heat-killed *E. coli* (HK-*E. coli*), which lacks certain molecules, is considered a low-quality food that is unable to support animal growth [24,25]. Morevoer, through metabolic-seq analysis, we identified significant changes in a large numbers of metabolites (Figure S1A, Table S1)，including lipids (Figure S1B, Table S1)，amino acid and their metabolites (Figure S1C, Table S1), as well as coenzymes and vitamins (Figure S1D, Table S1). Interestingly, we observed a significant decrease in carboxylic acids and their derivatives (Figure S1E, Table S1) in *E. coli* after being heat-killed (Figure S1F, Table S1). This suggests that HK-*E. coli* is nutritionally deficient for *C. elegnas* when compared to normal *E. coli* food.

87

88 Next, we conducted two behavior assays to facilitate the analysis of the food
89 evaluation process in animals by seeding L1 animals in assay plates (Figure
90 1A and 1B). In the avoidance assay, wild-type animals avoided the HK-*E. coli*
91 food (Figure 1A). Interestingly, in the food choice assay, animals initially showed
92 no preference between the two types of food (1-2h), but eventually exhibited a
93 preference for high-quality food (Live *E. coli*) up until the17h mark (Figure 1B,
94 Figure S1H). This suggests that worms depart from the HK-*E. coli* after
95 recognizing it as low-quality food source through ingestion.

96

97 In order to investigate the pathways in animals that response to HK-*E. coli*, we
98 performed transcriptomics analysis on worms that were cultured with both HK-
99 *E. coli* and Live *E. coli*. Gene-expression profiling revealed that stress response
100 genes, including those related to biotic stimulus, immune response and
101 response to stress, are up-regulated in animals fed with HK-*E. coli* (Figure 1C,
102 Table S2). Among these up-regulated genes, we identified 11 out of 62 of
103 UPR^{ER} target genes (Figure 1D, Figure S1G and Table S2). Additionally, about
104 50%-80% of up-regulated genes overlap with genes responding pathogenic
105 bacteria [26,27] (Figure 1E, Table S2), suggesting that UPR^{ER} and immune
106 pathways may responded to low-quality food. Consistent with the results of the
107 RNA sequencing (RNA-seq) analysis, the UPR^{ER} reporter (*Phsp-4::GFP*) and
108 immunity reporter (*Pirg-5::GFP*) were strongly induced under HK-*E. coli*
109 feeding condition (Figure 1F and 1G). Moreover, UPR^{Mt} reporter (*Phsp-6::GFP*)
110 was weakly induced under HK-*E. coli* feeding condition (Figure S1I), and
111 starved worm did not induce UPR^{ER} and immunity (Figure S1J and S1K).

112

113 Together, these findings suggest that low-quality food (HK-*E. coli*) triggers a
114 stress response pathway in animals, including UPR^{ER} and innate immune. This
115 implies that animals may assess the quality of food through UPR^{ER} and innate
116 immune pathway.

117

118 **Animals evaluate food quality through UPR^{ER}-immune depended**
119 **physiological food quality evaluation system**

120

121 To determine whether the UPR^{ER} and innate immune pathways play a role in
122 evaluating low-quality food, we first examined whether the activation of the
123 UPR^{ER} by HK-*E. coli* was dependent on the known signaling components of the
124 UPR^{ER} branches, including IRE/XBP-1, PERK/ATF-4 and ATF-6 [28,29]. We
125 observed no difference in *Phsp-4::GFP* induction with *atf-4* (Figure S2A and
126 S2J) or *atf-6* (Figure S2B and S2J) RNAi-mediated knockdown in animals fed
127 with HK-*E. coli*. However, knockdown of *ire-1/xbp-1* or mutation of *xbp-1*
128 reduced GFP fluorescence (Figure 2A, 2B and S2J). Among the 11 deferentially
129 expressed UPR^{ER} target genes in animals fed with HK-*E. coli* from RNA-seq
130 (Figure 1D), 64% of the genes are IRE-mediated genes (Figure S1G, Table S2).
131 The mRNA level of IRE-1-mediated splicing of *xbp-1* is also induced in animals
132 fed with HK-*E. coli* (Figure S2C). These data suggest that activation of the
133 UPR^{ER} by low-quality food depends on the IRE-1/XBP-1.

134

135 To further analyze whether XBP-1-dependent UPR^{ER} activation is critical for
136 animals to leave low-quality food, we tested food avoidance behavior using *xbp-*
137 *1* mutant. The results show that *xbp-1* mutants had a significantly decreased
138 likelihood of leaving of HK-*E. coli*, which was rescued by expressing *xbp-1* in
139 neuron rather than intestine (Figure 2C). This indicats that XBP-1-dependent
140 UPR^{ER} activation in neuron is critical for animals to evaluate low-quality food.

141

142 We then investigated which innate immune pathway is involved in evaluating
143 low-quality food. First, we analyzed HK-*E. coli* induced genes from RNA-seq.
144 Among these up-regulated genes, 82 out of 409 of PMK-1-dependent genes [30]
145 were identified (Figure S2D, Table S2). Second, we confirmed the induction of
146 several well-known PMK-1 target genes in RNA-seq data[31] (Figure S2E) and

147 reporter analysis (Figure S2F and S2G). Moreover, the induction of *Pirg-5::GFP*
148 was abolished in *pmk-1* knockdown animals fed with HK-*E. coli* (Figure 2D and
149 S2K). Third, we found that the phosphorylated PMK-1 (p-PMK-1) level was
150 prominently increased in wild-type N2 animals fed HK-*E. coli* compared to
151 feeding *E. coli* OP50 (Figure 2E). Finally, *pmk-1* mutants had a decreased
152 likelihood of leaving of HK-*E. coli*, which was rescued by expressing *pmk-1* in
153 neurons rather than intestine (Figure 2F). These data suggest that PMK-1
154 regulated immune pathway evaluates low-quality food, especially the neuronal
155 PMK-1 has a critical function for food quality response.
156
157
158 **XBP-1 and PMK-1 are in the same pathway for evaluating food quality**
159
160 Next, we explored the connection between UPR^{ER} (IRE-1/XBP-1) and innate
161 immunity (PMK-1 p38 MAPK) in food quality evaluation. We found that *Pirg-*
162 *5::GFP* induction (Figure S2H and S2K) and PMK-1 activation (Figure 2E) were
163 decreased in animals with *xbp-1* mutation or knockdown when fed with HK-*E.*
164 *coli*, suggesting that XBP-1 could regulate PMK-1 under this condition.
165 Additionally, *Phsp-4::GFP* induction under HK-*E. coli was* not affected in
166 animals with *pmk-1* RNAi (Figure S2I), indicating that XBP-1-dependent UPR^{ER}
167 activation is not regulated by PMK-1. Finally, we constructed a double mutant
168 of *xbp-1* and *pmk-1* and found that the food avoidance phenotype of the double
169 mutant was similar to the *pmk-1* mutant (Figure 2G), indicating that PMK-1 is
170 downstream of XPB-1 in responding to low-quality food.
171
172
173 **Sugar deficiency in HK-*E. coli* food induces stress response and**
174 **avoidance behavior in animals**
175
176 We then investigated which nutrients/metabolites are sensed by animals

177 through the XBP-1-PMK-1 axis for food quality evaluation. First, we
178 hypothesized that the nutrition status is improved in *E. coli* mutant (HK-
179 treatment), which could inhibit URP^{ER} and immune response in animals (Figure
180 S3A). We established a system for screening the *E. coli* mutant keio library
181 (Figure S3A), and identified 20 *E. coli* mutants that did not induce *hsp-4::GFP*
182 through the UPR^{ER} reporter (*irg-5::GFP*) after three rounds of screening (Table
183 S3). From these 20 E. coli mutant, we identified 9 *E. coli* mutants that did not
184 induce *irg-5::GFP* through the immunity reporter (*irg-5::GFP*) screening (Figure
185 S3B, S3C, Table S3). Animals fed HK-*yfbR*, which catalyzes carbohydrate
186 derivative metabolic process[32], had a decreased ability to leave food (Figure
187 3A, Table S3), indicating that HK-*yfbR* may be a higher quality food for animals
188 compared to HK-K12.
189
190 Secondly, we preformed a metabolomics analysis of different quality food (HK-
191 K12, HK-*yfbR* and Live-K12). We found that the level of 13 metabolites were
192 similar between HK-*yfbR* and Live-K12, but significantly changed in HK-K12
193 (Figure 3B, Figure S3D, and Table S1). We also found that genes involved in
194 glycolysis/gluconeogenesis were up-regulated in animals fed with HK-*E. coli*
195 (Figure S3E), suggesting that glycolysis/gluconeogenesis metabolism is
196 disordered in animals fed with HK-*E. coli,* which may result from changes in
197 sugar/carbohydrate intake. The carbohydrates (D-trehalose, Lactose, and D-
198 (+)-sucrose) were also decreased in HK-*E. coli* (Figure 3B), suggesting that
199 carbohydrate deficiency may induce stress response and avoidance behavior
200 in animals.
201
202 Thirdly, to determine which carbohydrate inhibits stress response in animals,
203 we supplemented each metabolite to HK-*E. coli* and found that only Lactose,
204 and D-(+)-sucrose inhibited HK-*E. coli* induced UPR^{ER} (Figure 3C and 3D,
205 Figure S3F). Moreover, we found from our metabolomic data that the sugar
206 level, including Lactose, and D-(+)-sucrose, and D-(+)-Glucose, was also

207 decreased in HK-*E. coli* (Figure 3B, Table S1). Since Lactose and D-(+)-sucrose
208 are hydrolyzed to produce glucose[33,34], we wondered whether glucose also
209 inhibits the stress response in animals. We found that D-(+)-Glucose
210 supplementation also inhibited HK-*E. coli* induced UPR^{ER} (Figure 3E), immune
211 response (Figure 3F, 3G and Figure S3G) and avoidance (Figure 3H). Moreover,
212 sugar supplementation did not affect UPR^{ER} and immunity in normal food
213 (OP50) or starved condition (NGM) (Figure S3H and S3I).
214
215 Together, these findings suggest that sugar/carbohydrates deficiency in HK-*E.*
216 *coli* induces a stress response and avoidance behavior in animals, which can
217 be inhibited by D-(+)-Glucose supplementation. This implies that animals may
218 evaluate the sugars deficiency through the activation of UPR^{ER} and immune
219 responses.
220
221
222 **Animals could overcome a low-quality food environment by sugar**
223 **supplementation through vitamin C biosynthesis**
224
225 We discovered that D-(+)-Glucose supplementation inhibited HK-*E. coli*
226 induced UPR^{ER} (Figure 3E), immune response (Figure 3F, 3G and Figure S3G)
227 and avoidance (Figure 3H). Simultaneously, vitamin C (VC), which is
228 synthesized by glucuronate pathway using D-Glucose [35,36] (Figure 4A), was
229 found contribute to neuroprotective[37,38], immune defense[39,40], and inhibits
230 inflammatory and ER stress[41,42]. This led us to question whether the Vitamin C
231 biosynthesis pathway is involved in evaluating low-quality food by using D-
232 Glucose.
233
234 Firstly, we observed an increase in the vitamin C level in animals when fed with
235 HK-yfbR (Figure 4B), a high carbohydrate food compared to HK-E. coli (Figure
236 3B and Figure S1E). However, the VC level in bacteria is same (Figure S4A).

237 The VC level also increased when D-Glucose (Figure S4B) or D-glucuronate
238 (D-GlcA) was added to HK-*E. coli* (Figure 4C), which was abolished by
239 knocking down VC biosynthesis genes (Figure 4C and S4B). This suggests that
240 additional of sugar supplementation promotes VC synthesis in animals fed with
241 HK-*E. coli.*
242
243 Secondly, we hypothesized that animals could overcome a low-quality food
244 (HK-*E. coli*) environment by inhibiting the stress response through increasing
245 vitamin C biosynthesis. We found that VC or D-glucuronate (D-GlcA)
246 supplementation inhibited HK-*E. coli* induced UPR^{ER} (Figure 4D), immune
247 response including *irg-5/sysm-1* reporter expression (Figure 4E and Figure
248 S4C) and p-PMK-1 (Figure 4F and 4G), as well as food avoidance (Figure 4H).
249
250 Finally, we asked whether inhibition of stress response and avoidance by sugar
251 supplementation depends on the vitamin C biosynthesis pathway. We found
252 that suppression of HK-*E. coli* induced UPR^{ER} (Figure 4I), immune response
253 (Figure 4J and Figure S4D) and food avoidance (Figure 4K) by D-GlcA/sugar
254 supplementation was abolished in animals with RNAi of VC biosynthesis genes.
255 Food selection behavior assays showed that D-GlcA/sugar supplementation
256 increased the preference for heat-killed bacteria, which was also suppressed
257 by knocking down VC biosynthesis genes (Figure S4E). However, VC
258 supplementation still suppressed the UPR^{ER} (Figure 4I), immune response
259 (Figure 4J and Figure S4D) and food avoidance (Figure 4K), and increased the
260 food preference (Figure S4E) in animals with or without RNAi of VC
261 biosynthesis genes. This suggests that VC, as the final metabolite synthesized
262 from D-Glucose, is critical for low-quality food response in animals.
263
264 Together, these data indicate that the Vitamin C biosynthesis pathway is
265 critical for evaluating whether food is of higher quality and can be eaten by
266 animals. It also suggests that animals could improve their VC levels to adapt to

267 bad food environment.

268

269 **Animals evaluate sugar and vitamin C through neuronal XBP-1 and PMK-**
270 **1**

271 As D-GlcA/sugar and VC supplementation suppressed HK-*E. coli* induced
272 UPR^{ER}, immune response and food avoidance behavior, we investigated
273 whether animals evaluate sugar and VC through XBP and PMK-1 dependent
274 pathways. We performed a food selection behavior assay by adding D-Glc, D-
275 GlcA or VC to the NGM, *E. coli* and HK-*E. coli* (Figure 5A). The food selection
276 behavior assays revealed that supplementation with D-Glc, D-GlcA, or VC
277 inhibits the animals' choice of sugar or VC on *E. coli*-OP50 feeding conditons
278 (Figure S4F). This suggests that supplementation with D-Glc, D-GlcA, or VC
279 may alter the metabolites of live bacteria, leading to avoidance by the animals.
280 There was no preference observed on NGM (no food condition)
281 supplementation with D-Glc and VC (Figure S4G), indicating that the intake of
282 sugar or VC alone does not influence animal preference. However, alone D-
283 GlcA could influence worm physiology which induces preference change
284 (Figure S4G). Interestingly, D-Glc and D-GlcA (Figure 5B and 5C) or VC (Figure
285 5D) supplementation increased the preference for heat-killed bacteria, which
286 was suppressed in *xbp-1* or *pmk-1* mutant animals. However, this preference
287 was also rescued in *xbp-1* or *pmk-1* mutant animals by expressing XBP-1 or
288 PMK-1 in neurons rather than intestine (Figure 5B-D), indicating that neuronal
289 XBP-1 and PMK-1 are critical for physiological food elevation system for
290 monitoring the level of sugar and VC under low-quality food condition.

291

292

293

294 **Discussion**

295

296 To better survive, animals must evolve a system to recognize and evaluate the

297 quality of their food. This includes the sensory neuron evaluation system for
298 immediate response and feeding decision [2], as well as physiological food
299 evaluation system for chronic response to ingested food. In our previous study,
300 we discovered that the TORC1-ELT-2 pathway, acting as master regulators in
301 intestine, evaluates vitamin B2 deficiency in low-quality food (HK-*E. coli)* and
302 regulates gut digestive activity to impact animal's food behavior [24]. To further
303 identified the mechanism by which animals evaluate low-quality food (HK-*E.*
304 *coli*), we performed metabolomics and transcriptomics analyses to identify
305 specific nutrition deficiencies in low-quality food and the cellular response
306 pathways that are involved in food evaluation pathway. This study identified a
307 physiological food evaluation mechanism by which animals detect sugar (in
308 food) and vitamin C (in animals) deficiency through UPR^{ER} (IRE-1/XBP-1) -
309 Innate immunity (PMK-1/p38 MAPK) regulated cellular stress response
310 program in neurons that dictates food avoidance and selection behaviors.
311
312 Unlike the sensory neuron evaluation system, which permits rapid feeding
313 decisions through smell and taste, the cellular stress response as physiological
314 food evaluation system describe here requires a slow and multi-step signal
315 transduction process after the ingestion of food. The disruption of cellular
316 homeostasis by ingested of low-quality or toxic food can activate stress
317 response mechanisms that both increase the cellular ability to withstand and
318 adapt to this disruption of homeostasis and promote behavioral strategies to
319 avoid these conditions and lessen their impact on the organism. These cellular
320 stress response mechanisms include heat shock response, unfolded protein
321 response, oxidative stress response [43]. Therefore, this slow physiological food
322 evaluation system is an evolutionary adaptation mechanism for detecting
323 nutrition deficiencies in food that was not detected by quick sensory neuronal
324 system.
325

326 One of cellular stress response, UPR^{ER}, is activated by stresses such as
327 infection and nutrition deficiency that affect homeostasis in the endoplasmic
328 reticulum (ER) [28]. The activation of the UPR^{ER} by expression of *xbp-1s* in the
329 nervous system has recently been shown to promote changes in feeding and
330 foraging behavior [44]. The p38 PMK-1 pathway regulates the expression of
331 secreted innate immune effectors and is required for survival during infection [45].
332 Moreover, UPR^{ER} and innate immunity increased by disrupting in vivo state
333 would induce worm aversion from food lawn[46-49]. Thus, these two cellular stress
334 response pathways are critical for animals' survival in changing environment.
335 However, whether UPR^{ER} (IRE-1/XBP-1) - Innate immunity (PMK-1/p38 MAPK)
336 evaluates food quality under physiological conditions is largely unexplored. Our
337 study presents evidence that low-quality food (HK-*E. coli*) activate UPR^{ER} and
338 PMK-1, and promotes animals to leave food. It is independent of avoidance
339 behavior of hyperactivation of kgb-1/MAPK pathway[49] (Figure S4H). Mover, our
340 study also shows that neuronal UPR^{ER} and PMK-1 are critical for evaluating
341 low-quality food. Therefore, our study established a novel physiological food
342 evaluation system by activating the cellular stress response program with
343 UPR^{ER} (IRE-1/XBP-1) - Innate immunity (PMK-1/p38 MAPK).
344
345 Collectively, this study uncovers the unexpected function of UPR^{ER} (IRE-1/XBP-
346 1) - Innate immunity (PMK-1/p38 MAPK) as a physiological food evaluation
347 system for evaluating and sensing food quality in animals. It also highlights the
348 utility of the HK-*E. coli* (low-quality food) - *C. elegans* interaction as a means to
349 dissect the mechanism of food evaluation system in assessing food. Most
350 importantly, it reveals that animals are capable of altering their nutrient (Vitamin
351 C) levels through in vivo synthesis or food intake to adapt to a poor food
352 environment when better food choices are not available.
353
354 **Author Contributions**
355 P. L designed, performed experiments, analyzed data. X. L constructed all

356 transgenic animals. B.Q. designed research, supervised this study, and wrote
357 the paper with inputs from P. L.
358

359 **Acknowledgments**
360 We thank the Caenorhabditis Genetics Center (CGC) (funded by NIH
361 P40OD010440) for strains; Dr. Zhao Shan for suggestions. This work was
362 supported by the Ministry of Science and Technology of the People's Republic
363 of China (2019YFA0803100，2019YFA0802100), the National Natural Science
364 Foundation of China (32170794), Yunnan Applied Basic Research Projects
365 (202001AV070011, 202001AW070006, 202201AT070196), the Yunnan
366 University Startup Program.
367

368 **Declaration of interests**
369 The authors declare no competing interests.
370

371 **Main Figure Legends**

372 **Figure 1. The stress response is induced in animals fed low-quality food,**
373 **HK-*E. coli*.**

374 (A) Schematic drawing and quantitative data of the food aversion assay. Circles
375 indicate the food spot for live (yellow) and HK-OP50 (red) bacteria, respectively.
376 The animals were scored 16-17 hours after L1 worms were placed on the food
377 spot. Data are represented as mean ±SD from three independent experiments，
378 79-129 animals/assay.

379 (B) Schematic method and quantitative data of the food selection assay. Live
380 (yellow), heat-killed (red) *E. coli* and LB as the buffer for *E. coli* were placed on
381 indicated position. Synchronized L1 worms were place in the center spot. The
382 selection index was calculated at the indicated time. Data are represented as
383 mean ±SD from eight independent experiments, 123-792 animals/assay.

384 (C) GO enrichment analysis of up-regulated genes in animals fed with HK-*E.*
385 *coli* vs live *E. coli*.

386 (D) Venn diagram showing numbers of UPR^{ER} target genes and up-regulated
387 genes in animals fed HK-*E. coli*, and their overlap.

388 (E) Venn diagram showing numbers of induction genes by four pathogenic
389 bacteria and HK-*E. coli* induced genes, and their overlap. The gene expression
390 data was extracted from published data of animals' infection with Pseudomonas
391 aeruginosa (PA) [26], Bacillus thuringiensis (Bthu) [27], Staphylococcus aureus
392 (Saur) [27], and Serratia marcescens (Smar) [27].

393 (F-G) GFP fluorescence images and bar graph showing that *Phsp-4::GFP* (F)
394 and *Pirg-5::GFP* (G) were induced in animals fed wiht HK-*E. coli.* n is the
395 number of worms scored from at least three independent experiments. Data
396 are represented as mean ± SD.

397 For all panels, Scale bar shows on indicated figures, 50 μm. * $p<0.05$, **
398 $p<0.01$, *** $p < 0.001$, **** $p<0.0001$, ns: no significant difference. Precise P
399 values are provided in Raw Data.

400 **Figure 2. Animals evaluate food quality through UPRER (ire-1/xbp-1) -**
401 **Innate immunity (pmk-1 MAPK) axis.**

402 (A-B) GFP fluorescence images and bar graph showing that HK-*E. coli* induced
403 *Phsp-4::GFP* was decreased in animals with *ire-1* or *xbp-1* RNAi treatment (A)
404 or *xbp-1* mutation (B). n is the number of worms scored from at least three
405 independent experiments. Data are represented as mean ± SD.

406 (C) Food aversion assay showing that *xbp-1* mutation eliminated the
407 discrimination against HK-*E. coli.* However, this effect is rescued by expressing
408 *xbp-1* in neurons rather than intestine. Data are represented as mean ±SD from
409 five independent experiments, 156-763 animals/assay.

410 (D) GFP fluorescence images and bar graph showing that HK-*E. coli* induced
411 *Pirg-5::GFP* was decreased in animals with *pmk-1* RNAi treatment. n is the
412 number of worms scored from at least three independent experiments. Data
413 are represented as mean ± SD.

414 (E) Western blot images showing the level of p-PMK-1 in L1 animals (Wild-type
415 N2 and *xpb-1* mutant) fed with OP50 or HK-OP50 for 4 h. The level of p-PMK-
416 1 is induced in animals fed HK-OP50.

417 (F) Food aversion assay showing that *pmk-1* mutation eliminated the
418 discrimination against HK-*E. coli.* However, this effect is rescued by expressing
419 *pmk-1* in neurons rather than intestine. Data are represented as mean ±SD
420 from five independent experiments, 168-492 animals/assay.

421 (G) Food aversion assay in wild-type, *xbp-1*, *pmk-1* and double mutant. Data
422 are represented as mean ±SD from five independent experiments, 259-490
423 animals/assay..

424 For all panels, Scale bar shows on indicated figures, 50 μm. * $p<0.05$, **
425 $p<0.01$, *** $p < 0.001$, **** $p<0.0001$, ns: no significant difference. Precise P
426 values are provided in Raw Data.

427 **Figure 3. *HK-E. coli* is low sugar food, which induce stress response and**
428 **avoidance behavior in animals.**

429 (A) Food aversion assay showing that wild-type animals eliminated the
430 discrimination against HK-*E. coli* when *yfbR* is mutated in *E. coli*. Data are
431 represented as mean ±SD four independent experiments, 251-490
432 animals/assay.

433 (B) Heat map showing the thirteen differential metabolites from HK-K12, HK-
434 *yfbR*, and K12 in 4 independent experiments. Color indicates the relative level
435 of each metabolite.

436 (C-D) The bar graph showing that HK-*E. coli* induced *Phsp-4::GFP* was
437 decreased in animals with lactose (C) or D-(+)-sucrose (D) supplementation. n
438 is the number of worms scored from at least three independent experiments.
439 Data are represented as mean ± SD.

440 (E-F) GFP fluorescence images and bar graph showing that HK-*E. coli* induced
441 *Phsp-4::GFP* (E) and *Pirg-5::GFP* (F) were decreased in animals with D-(+)-

442 Glucose (D-Glc) supplementation. n is the number of worms scored from at
443 least three independent experiments. Data are represented as mean ± SD.

444 (G) Western blot images showing the level of p-PMK-1 in L1 animals fed HK-*E.*
445 *coli* with or without D-(+)-Glucose (D-Glc) supplementation for 4 h. The level of
446 p-PMK-1 is decreased in animals fed HK-OP50+D-Glc.

447 (H) Food aversion assay showing that wild-type animals eliminated the
448 discrimination against HK-*E. coli* with D-Glc supplementation. Data are
449 represented as mean ±SD six independent experiments, 190-492
450 animals/assay.

451 For all panels, Scale bar shows on indicated figures, 50 μm. * $p<0.05$, **
452 $p<0.01$, *** $p < 0.001$, **** $p<0.0001$, ns: no significant difference. Precise P
453 values are provided in Raw Data.

454

455 **Figure 4. Vitamin C biosynthesis pathway is critically involved in**
456 **evaluating sugar in the food**
457 (A) Cartoon illustration of a simplified, Vitamin C biosynthesis pathway in *C.*
458 *elegans*. The relevant coding genes of enzymes was labeled with red.
459 (B) The level of total L-ascorbic acid (TAA) in animals fed with Live-K12, HK-
460 K12, or HK-yfbR. Data are represented as mean ±SD from six independent
461 experiments.
462 (C) The level of total L-ascorbic acid (TAA) in animals (control or knockdown of
463 Vitamin C biosynthesis genes) fed with HK-*E. coli* with or without D-glucuronate
464 (D-GlcA) supplementation. Data are represented as mean ±SD from eight
465 independent experiments.

466 (D-E) GFP fluorescence images and bar graph showing that HK-*E. coli* induced
467 *Phsp-4::GFP* (C) and *Pirg-5::GFP* (D) were decreased in animals with D-GlcA
468 or Vitamin C supplementation. n is the number of worms scored from at least
469 three independent experiments. Data are represented as mean ± SD.

470 (F-G) Western blot images showing the level of p-PMK-1 in L1 animals fed with
471 HK-*E. coli* with D-GlcA or Vitamin C supplementation for 4 h. The level of p-
472 PMK-1 is decreased in animals with D-GlcA (F) or Vitamin C (G)
473 supplementation.

474 (H) Food aversion assay showing that wild-type animals eliminated the
475 discrimination against HK-*E. coli* with D-GlcA or Vitamin C supplementation. N
476 is number of independent experiments. Data are represented as mean ±SD
477 from four independent experiments, 153-292 animals/assay.

478

479 (I-K) The bar graph showing that suppression of HK-*E. coli* induced *Phsp-*
480 *4::GFP* (I), *Pirg-5::GFP* (J) and food avoidance (K) by D-GlcA supplementation
481 was abolished in animals with RNAi of VC biosynthesis genes, which was not
482 affect by Vitamin C supplementation. n is the number of worms scored from at
483 least three independent experiments and Data are represented as mean ±SD(I-
484 J). Data are represented as mean ±SD from five independent experiments, 252-
485 537 animals/assay (K).

486 For all panels, Scale bar shows on indicated figures, 50 μm. * $p<0.05$, **
487 $p<0.01$, *** $p < 0.001$, **** $p<0.0001$, ns: no significant difference. Precise P
488 values are provided in Raw Data.

489

490 **Figure 5. Animals evaluate sugar and vitamin C through neuronal XBP-1**
491 **and PMK-1**

492 (A) Schematic method of the food selection assay. Heat-killed *E. coli* (red) and
493 HK-*E. coli* with chemical supplementation (green) were placed on indicated
494 position. Synchronized L1 worms were then place in plate. After 16-17hs, the
495 selection index was calculated.

496 (B-D) Food selection assay showing that *xbp-1* or *pmk-1* mutation eliminated
497 the preference of HK-*E. coli* with D-Glc (B), D-GlcA (C) or Vitamin C (D)
498 supplementation, which was rescued in *xbp-1* or *pmk-1* mutant animals by

499 expressing XBP-1 or PMK-1 in neurons rather than intestine.

500 Data are represented as mean ±SD from five independent experiments, 68-647
501 animals/assay (B).

502 Data are represented as mean ±SD from six independent experiments, 83-701
503 animals/assay (C).

504 Data are represented as mean ±SD from six independent experiments, 67-
505 1035 animals/assay (D).

506 For all panels, Scale bar shows on indicated figures, 50 μm. * $p<0.05$, **
507 $p<0.01$, *** $p < 0.001$, **** $p<0.0001$, ns: no significant difference. Precise P
508 values are provided in Raw Data.

509 **Figure 6. Schematic model of physiological food evaluation system in**
510 **evaluating/sensing sugar and vitamin C through UPR^{ER} (IRE-1/XBP-1) -**
511 **Innate immunity (PMK-1/p38 MAPK) axis.**

512 Vitamin C level is low in animals fed low sugar food, HK-*E. coli*. Sugar and
513 Vitamin C deficiency activate cellular UPR^{ER} and immune response, which
514 promote animals to leave low-quality food and seek better food for survival. This
515 cellular stress regulated physiological food evaluation system depends UPR^{ER}
516 (IRE-1/XBP-1) - Innate immunity (PMK-1/p38 MAPK) axis in neuron.

517

518 **<u>Supplemental Figure legends</u>**

519

520 **Figure S1. Food selection assay of animals fed HK-*E. coli* or *E. coli.***
521 **Relative to Figure 1.**

522 (A-E) Metabolomics analysis of different quality food (HK-K12, HK-*yfbR* and
523 Live-K12). Cluster analysis of all metabolites (A), lipids and their derivatives (B),
524 amino acids and their derivatives (C), coenzymes and vitamins (D), and
525 carbohydrates and their derivatives (E) from Live-K12, HK-K12, and HK-yfbR.

526 Color indicates the relative level of each metabolite. HK-K12: heat-killed *E. coli*
527 wild-type K12; HK-*yfbR:* heat-killed *E. coli mutant yfbR;* K12: live *E. coli* wild-
528 type K12. z-score for standardizing data, complete for bi-clustering algorithm,
529 and Euclidean for distance method.
530 (F) Principal component analysis to test the repeatability of the metabolic
531 experiment. HK-K12: heat-killed *E. coli* wild-type K12; HK-yfbR: heat-killed *E.*
532 *coli* mutant yfbR; K12: live *E. coli* wild-type K12. LB: LB buffer for culturing *E.*
533 *coli.*
534 (G) GO enrichment analysis of UPR^{ER} dependent IRE-1 branch.
535 (H) The number of worms in each position calculated at the indicated time,
536 indicating that animals initially select both foods (1-2h), but eventually favor
537 high-quality food (Live E. coli) until 17h.
538 (I) UPR^{mt} Reporter (*Phsp-6:GFP*) was weakly induced in animals fed with HK-
539 E. coli
540 (J) UPR^{ER} Reporter (Phsp-4:GFP) expression in animals under normal food
541 (OP50), low quality food (HK-OP50), and starved (M9: hatching L1 worm in M9,
542 NGM) condition;
543 (K) Immunity Reporter (Pirg-5:GFP) expression in animals under normal food
544 (OP50), low quality food (HK-OP50), and starved (M9: hatching L1 worm in M9,
545 NGM).
546 For all panels, Scale bar shows on indicated figures, 50 μm. * $p<0.05$, **
547 $p<0.01$, *** $p < 0.001$, **** $p<0.0001$, ns: no significant difference. Precise P
548 values are provided in Raw Data.
549

550 **Figure S2. UPRER and Innate immunity pathway in animals are critical for**
551 **evaluating HK-*E. coli*. Relative to Figure 2.**

552 (A-B) GFP fluorescence images and bar graph showing that HK-*E. coli* induced
553 *Phsp-4::GFP* was not affected in animals with *atf-4* (A) or *atf-6* (B) RNAi
554 treatment. n is the number of worms scored from at least three independent
555 experiments. Data are represented as mean ± SD.

556 (C) qPCR showing that IRE-1-mediated splicing of *xbp-1* mRNA is induced in
557 animals fed with *HK-E. coli.*

558 (D) Venn diagram showing the numbers of PMK-1 dependent genes [30] and up-
559 regulated genes in animals fed HK-*E. coli,* and their overlap.

560 (E) The expression of PMK-1 dependent genes which was extracted from RNA-
561 seq data from animals fed with *HK-E. coli*. The data from average of three
562 independent experiments (N=3)

563 (F-G) GFP fluorescence images and bar graph showing that *Psysm-1::GFP* (F)
564 and *Pirg-1::GFP* (G) were induced in animals fed *HK-E. coli.* n is the number of
565 worms scored from at least three independent experiments. Data are
566 represented as mean ± SD.

567 (H) GFP fluorescence images and bar graph showing that HK-*E. coli* induced
568 *Pirg-5::GFP* was decreased in animals with *ire-1* or *xbp-1* RNAi treatment. n is
569 the number of worms scored from at least three independent experiments. Data
570 are represented as mean ± SD.

571 (I) GFP fluorescence images and bar graph showing that *Phsp-4::GFP* was not
572 affected in animals with *pmk-1* RNAi treatment. n is the number of worms
573 scored from at least three independent experiments. Data are represented as
574 mean ± SD.

575 (J) UPR^{ER} Reporter (Phsp-4::GFP) expression in animals with candidate
576 RNAi feeding OP50 or HK-OP50

577 (K) immunity Reporter (Pirg-5::GFP) expression in animals with candidate
578 RNAi feeding OP50 or HK-OP50

579 For all panels, Scale bar shows on indicated figures, 50 μm. * $p<0.05$, **
580 $p<0.01$, *** $p < 0.001$, **** $p<0.0001$, ns: no significant difference. Precise P
581 values are provided in Raw Data.

582

583 **Figure S3. Low sugar food, HK-*E. coli*, induce stress response and**
584 **avoidance behavior in animals. Relative to Figure 3.**

585 (A) Flow chart of strategy for *E. coli* keio mutant screening. We identified 20 *E.*
586 *coli* mutants that did not induce *hsp-4::GFP* through the UPR^{ER} reporter (*irg-*
587 *5::GFP*) after three rounds of screening (Table S3). From these 20 E. coli
588 mutant, we identified 9 *E. coli* mutants that did not induce *irg-5::GFP* through
589 the immunity reporter (*irg-5::GFP*) screening (Table S3).

590 (B-C) The bar graph showing that HK-*E. coli* induced *Phsp-4::GFP* (B) and *Pirg-*
591 *5::GFP* (C) was decreased in animals fed mutant *E. coli* (Heat-killed). n is the
592 number of worms scored from at least three independent experiments. Data
593 are represented as mean ± SD.

(D) Venn diagram showing the number of deferentially metabolites in HK-*E. coli*-K12, HK-*E. coli-yfbR* and *E. coli*.

(E) KEGG enrichment analysis of deferentially expressed genes in animals fed HK-*E. coli* vs live *E. coli*. We noticed that all most of glycolysis/gluconeogenesis genes are up-regulated in animals fed HK-*E. coli*.

(F) The bar graph showing that HK-E. coli induced *Phsp-4::GFP* was not affected in animals with D-(+)-Trehalose supplementation. n is the number of worms scored from at least three independent experiments. Data are represented as mean ± SD. .

(G) GFP fluorescence images and bar graph showing that HK-*E. coli* induced *Psysm-1::GFP* was decreased in animals with D-(+)-Glucose (D-Glc) supplementation. n is the number of worms scored from at least three independent experiments. Data are represented as mean ± SD.

(H) UPR^{ER} Reporter (Phsp-4::GFP) expression animals with D-Glc supplementation under OP50, HK-OP50, or NGM condition.

(I) immunity Reporter (Pirg-5::GFP) expression animals with D-Glc supplementation under OP50, HK-OP50, or NGM condition.

For all panels, Scale bar shows on indicated figures, 50 μm. * $p<0.05$, ** $p<0.01$, *** $p < 0.001$, **** $p<0.0001$, ns: no significant difference. Precise P values are provided in Raw Data.

Figure S4. Vitamin C biosynthesis pathway is critically for evaluating low sugar. Relative to Figure 4.

(A) The level of total L-ascorbic acid (TAA) in Live-K12, HK-K12, or HK-yfbR. N is number of independent experiments. Data are represented as mean ±SD from six independent experiments.

(B) The level of total L-ascorbic acid (TAA) in animals fed HK-*E. coli* with or without D-Glc supplementation. Data are represented as mean ±SD from from eight independent experiments.

(C) GFP fluorescence images and bar graph showing that HK-*E. coli* induced *Psysm-1::GFP* was decreased in animals with D-GlcA or Vitamin C supplementation. n is the number of worms scored from at least three independent experiments. Data are represented as mean ± SD.

627 (D) The bar graph showing that suppression of HK-*E. coli* induced *Psysm-*
628 *1::GFP* by D-GlcA supplementation was abolished in animals with RNAi of VC
629 biosynthesis genes, which was not affect by Vitamin C supplementation. n is
630 the number of worms scored from at least three independent experiments. Data
631 are represented as mean ±SD.
632 (E) Food selection assay showing that the preference of HK-*E. coli* with D-GlcA
633 supplementation was abolished in animals by RNAi of Vitamin C biosynthesis
634 genes. Data are represented as mean ±SD from six independent experiments,
635 427-775 animals/assay.
636 (F) Food selection assay for OP50 & OP50 + + D-Glc, D-GlcA, or VC,
637 respectively. Data are represented as mean ±SD from five independent
638 experiments, 241-1182 animals/assay.
639 (G) Food selection assay for buffer & buffer + D-Glc, D-GlcA, or VC, respectively.
640 Data are represented as mean ±SD from five independent experiments, 8-153
641 animals/assay.
642 (H) Food avoidance assay for N2 & kgb-1 mutant animals fed with HK-E. coli.
643 Data are represented as mean ±SD from six independent experiments, 348-
644 660 animals/assay.
645 For all panels, Scale bar shows on indicated figures, 50 μm. * $p<0.05$, **
646 $p<0.01$, *** $p < 0.001$, **** $p<0.0001$, ns: no significant difference. Precise P
647 values are provided in Raw Data.
648
649 **Supplemental Tables:**
650 **Table S1.** Metabolices analysis. Relative to Figure S1A, S1B, S1C, S1D, S1E,
651 S1F, 3B, and S3D.
652 **Table S2.** RNA-seq analysis. Relative to Figure 1C, 1D, 1E, S1G, and S2D.
653 **Table S3.** Screening data for *E. coli* mutant keio library. Relative to Figure s
654 S3A, S3B, and S3C.
655 **Table S4.** Metabolomics-seq data of HK-K12, HK-yfbR and K12.
656 **Table S5.** RNA-seq data of animals fed with HK-*E. coli OP50* and *E. coli OP50.*

Raw-data. Raw data for experiments.

Star Methods

Resource Availability

Lead contact

Further information and requests for reagents may be directed to the Lead contact Bin Qi (qb@yun.edu.cn).

Materials availability

All reagents and strains generated by this study are available through request to the lead contact with a completed Material Transfer Agreement.

Data and code availability

Metabolomics-seq data are accessible in Table S4

RNA-seq data are accessible in Table S5.

This paper does not report original code.

Any additional information required to reanalyze the data reported in this paper is available from the lead contact upon request.

Experimental model and subject details

C. elegans strains and maintenance

Nematode stocks were maintained on nematode growth medium (NGM) plates seeded with bacteria (*E. coli OP50*) at 20℃.

1) The following strains/alleles were obtained from the Caenorhabditis Genetics Center (CGC) or as indicated:

N2 Bristol (wild type control strain);

AU78: agIs219 [*T24B8.5p::GFP::unc-54 3′ UTR + ttx-3p::GFP::unc-54 3′ UTR*];

687 SJ4005: *Phsp-4::GFP(zcIs4)*;

688 AY101: acIs101 [*F35E12.5p::GFP* + *rol-6(su1006)*]IG274: frIs7 [*nlp-29p::GFP* +

689 *col-12p::DsRed*] IV;

690 SJ17: *xbp-1 (zc12)*;

691 KU25: *pmk-1(km25)*;

692 AY102: *pmk-1(km25)* IV; acEx102 [*vha-6p::pmk-1::GFP* + *rol-6(su1006)*];

693 YNU108: Ex[*Prgef-1::pmk-1::GFP*；*Podr-1::RFP*][50];

694 *xbp-1(tm2482)* [51];

695 KU21：*kgb-1(km21)*;

696 AU133: *agIs17 [myo-2p::mCherry + irg-1p::GFP] IV;*

697 SJ4100: *zcIs13 [hsp-6p::GFP + lin-15(+)]*.

698 2)The following strains were constructed by this study:

699 YNU242: *xbp-1(tm2482); pmk-1(km25)* double mutant was constructed by

700 crossing: *xbp-1(tm2482)* with KU25[*pmk-1(km25)*].

701 YNU240: ylfEx149 [*xbp-1(tm2482); Prgef-1::xbp-1::GFP; Podr-1::RFP*]

702 transgene strain was constructed by injecting plasmid *Prgef-1::xbp-1::GFP* with

703 *Podr-1::RFP* in *xbp-1(tm2482)* background

704 YNU241: ylfEx150 [*xbp-1(tm2482); Pges-1::xbp-1::GFP; Podr-1::RFP*]

705 transgene strain was constructed by injecting plasmid Pges-1:xbp-1::GFP with

706 *Podr-1::RFP* in *xbp-1(tm2482)* background

707

708 **Bacterial strains**

709 *E. coli*-OP50, *E. coli-K12* (BW25113), and *E. coli-K12* mutant were cultured at

710 37˚C in LB medium. A standard overnight cultured bacteria was then spread

711 onto each Nematode growth media (NGM) plate.

712

713 **Method Details**

714

715 **Generation of transgenes**

716 1）To construct the *C. elegans* plasmid for expression of *xbp-1* in neuron,
717 3057bp promoter of *rgef-1* and genomic DNA of *xbp-1* was inserted into the
718 PPD95.77 vector. DNA plasmid mixture containing *Prgef-1::xbp-1::GFP*
719 (25ng/ul) and *Podr-1p:RFP* (25ng/ul) was injected into the gonads of adult *xbp-*
720 *1(tm2482)*.
721 2）To construct the *C. elegans* plasmid for expression of *xbp-1* in intestine,
722 2549 bp promoter of ges-1 and genomic DNA of xbp-1 was inserted into the
723 PPD95.77 vector. DNA plasmid mixture containing *Pges-1:xbp-1::GFP* (25ng/ul)
724 and *Podr-1p:RFP (25ng/ul)* was injected into the gonads of adult *xbp-1(tm2482)*.
725
726 **Preparation and feeding of worm food**
727 We followed an established protocol [24,25] to prepare heat-killed (HK) *E. coli*.
728 Briefly, a standard OD600=0.5-0.6 of *E. coli* OP50 and *E. coli* K12 grown in LB
729 broth was concentrated to 1/20 vol and was then heat-killed at 80℃ for 180
730 min. About 150ul of the heat-killed bacteria was spread onto each 35mm NGM
731 plate.
732
733 **Preparation of HK-*E. coli* + carbohydrate or Vitamin C food**
734 1) 100ul of water, 100ul of L-ascorbic acid (dissolved in water at a concentration
735 of 100mg/ml, Sangon Biotech, 100143-0100) or 100 ul of D-Glucuronic acid
736 (dissolved in water at a concentration of 100mg/ml，Adamas, 1102520) was
737 mixed with 500 ul of HK-*E. coli*, then 150ul of the mixture was spread onto
738 35mm NGM plates.
739 2) 12.5ul of water or 12.5ul of D-(+)-Glucose (dissolved in water at a
740 concentration of 100mg/ml, Sangon Biotech, A501991-0500) was mixed with
741 500 ul of HK-*E. coli*, then 150ul of the mixture was spread onto 35mm NGM
742 plates.
743
744 **Behavioral assay**
745 ***C. elegans* selection assays**

For *C.elegans* to have enough space to evaluate food, we add 18ul of the sample onto a 35mm NGM plate. This creates a round lawn with a radius of 0.5mm, which occupies about 8% of the total plate area.

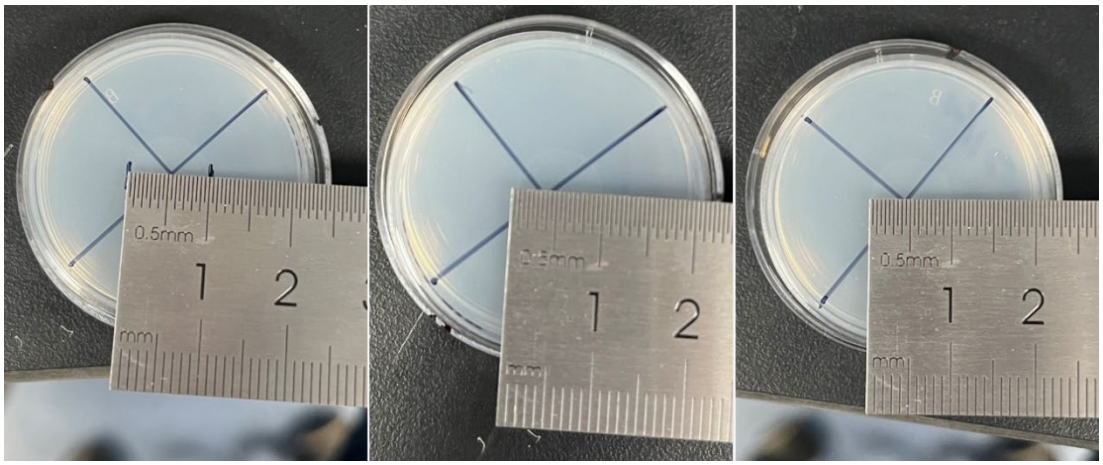

$$\frac{a}{b} = \frac{\pi r_1^2}{\pi \gamma_2^2} = \frac{0.5mm^2}{1.75mm^2} = 8\%$$

a: the area of bacterial lawn
b: the space of worm life (area of culture dish)

1) 18ul of heat-killed OP50, live OP50, and LB broth (as the buffer for bacteria) was added into 35mm NGM plate in an equilateral triangle pattern. Then, synchronized L1 worms were seeded in the center of NGM plate for 16-17h at 20℃ (as indicated in Figure1B).

2) 18ul of heat-killed OP50 and heat-killed OP50 with D-GlcA or Vitamin C was added into 35mm NGM plate in an equilateral triangle pattern., then synchronized L1 worms were seeded on equilateral triangle of NGM plate for 16-17h at 20℃ (as indicated in Figure 5A).

Here is Selection rate formula:

$$selection\ rate = \frac{\frac{worm\ amount}{one\ lawn\ area}}{\frac{worm\ amount}{lawn1\ area} + \frac{worm\ amount}{lawn2\ area} + \frac{worm\ amount}{lawn3\ area} \cdots}$$

C. elegans aversion assays

766 18ul food was spread out the center of NGM plate, then synchronized L1 worms
767 were seeded on center of food for 16-17h at 20℃.

768 $$\text{Aversion index } = \frac{worm\ amount\ of\ out\ \text{of}\ lawn}{worm\ amount\ of\ (out + in)\ lawn}$$

769 Three to ten replicates for each condition were performed for each assay, and
770 the experiments were duplicated on different days.
771

772 **Analysis of the fluorescence intensity in worms**

773 The synchronized L1 worms carrying either UPR^{ER} reporter (*Phsp-4::GFP*) or
774 innate immunity reporter (*Pirg-5::GFP*; Psysm-1p::GFP; *Pirg-1p::GFP*) were
775 seeded on NGM with indicated food and incubated for 24h at 20℃. For
776 fluorescence imaging, worms were anesthetized with 25 mM levamisole and
777 photographed using either an Olympus BX53 microscope or Olympus MVX10
778 dissecting microscope equipped with a DP80 camera.
779 The fluorescence intensity in entire intestinal region was quantified using
780 ImageJ software and normalized to the body area.
781

782 ***E. coli* Keio collection screen**

783 The whole Keio *E. coli* single mutant collection (Baba et al., 2006) was
784 screened. Mutant bacteria strains, as well as the wild-type control strain
785 BW25113, were cultured in LB medium with 50μg/ml kanamycin at 37℃until an
786 OD600 of 0.5-0.6 was reached. The bacteria were then heat-killed following our
787 established protocol [24], and 150 ul of the heat-killed the mutant *E. coli* was
788 spread onto 3.5 cm NGM plates. Synchronized L1 worms carrying UPR^{ER}
789 reporter (*Phsp-4::GPF*) were seeded and cultured for 24h at 20℃. The
790 fluorescence was then examined by using an Olympus MVX10 dissecting
791 microscope, progressive screening three times. next, an 4th screen was
792 performed using immune reporter (*Pirg-5::GPF*) animals fed with HK-E. coli
793 mutants that reduced the *Phsp-4::GPF* fluorescence. Finally, an aversion
794 behavior assay was performed using HK-*E. coli* mutants that both reduced

795 *Phsp-4::GPF* and *Pirg-5::GPF.* HK-*E. coli* mutants that reduced UPR^{ER},
796 immune and avoidance behavior were identified through this screening.
797
798 **RNAi treatment**
799 Bacterial clones from either the MRC RNAi library [52] or the ORF-RNAi Library
800 [53] were used. RNAi plates were prepared by adding IPTG to NGM agar to a
801 final concentration of 1 mM. Overnight *E. coli* cultures (LB broth containing 100
802 ug/ml ampicillin and 100uM IPTG) of specific RNAi strains and the control
803 HT115 strain were seeded onto RNAi feeding plates and cultured at room
804 temperature until adulthood. Synchronized L1 worms were treated RNAi by
805 feeding (Ahringer, Reverse genetics, WormBook 2006) for the first generation
806 and allowed to grow to maturity. The worms were then bleached and hatched
807 in M9 buffer for 18hr. The synchronized L1 worms were then seeded on the
808 indicated feeding plate.
809
810 **Western blot**
811 To measure the level of p-PMK-1, worms (feeding different food for 4h) were
812 analyzed by standard western blot methods and probed with anti-p38 (dilution
813 = 1:5,000; Cell Signaling, 9212S), anti-p-p38 (dilution = 1:5,000; Cell Signaling,
814 4511S) and anti-α-tubulin (dilution = 1:10,000; Sigma T5168) as a loading
815 control.
816
817 **Total content of ascorbic acid (TAA) assay**
818 The total content of ascorbic acid was measured using the kits (Beijing Biotech-
819 Pack-analytical Scientific Co., Ltd., Beijing, China, BKWB132 http://biotech-
820 pack-analytical.foodmate.net/) according to the manufacturer's protocol. Briefly,
821 L1 worms were seeded on the different feeding assay plate and cultured for 4
822 hours. The worms were then lysed in ice-cold conditions using lysis buffer.
823 Equal amounts of protein were used for the normalization. Here is formula for
824 getting TAA concentration

825 $$\mathrm{TAA(ug/mg\ prot)} = ((\triangle \mathrm{A} - \mathrm{a}) \div \mathrm{b})) \div (\mathrm{Cpr} \times \mathrm{V1}) \times \mathrm{D}$$

826 V1 - the volume of supernatant of for experiment

827 Cpr – the concentration of supernatant protein

828 D – Dilution ratio of supernatant

829 a – the intercept of standard curve

830 b – the slope of standard curve

831 the standard curve y = 0.0611x + 0.0003 for Figure 4C; y = 0.0258x + 0.0066

832 for Figure 4B, S4A and S4B.

833

834 **Preparation of samples for RNA sequencing**

835 RNA-seq was done with three biological replicates that were independently

836 generated, collected, and processed. Adult wild type (N2) worms were

837 bleached and then the eggs were incubated in M9 for 18 hours to obtain

838 synchronized L1 worms. L1 worms were cultured in the NGM plate with *HK-E.*

839 *coli* or *E. coli* for 4hrs at 20℃. L1 worms were then collected for sequencing.

840

841 **RNA sequencing and data processing**

842 For the RNA sequencing assay, cDNA libraries were constructed, and single-

843 end libraries were sequenced using the Illumina platform (Novogene, Beijing,

844 China). HISAT2 [54] was used to map the clean reads to the reference gene

845 sequence (Species: Caenorhabditis_elegans; Source: NCBI; Reference

846 Genome Version: GCF_000002985.6_WBcel235), and then “featureCounts”

847 tool in subread software [55] was used to calculate the gene expression level of

848 each sample. Read counts were inputted into DESeq2 [56]to calculate differential

849 gene expression and statistical significance. Differentially expressed genes

850 (DEGs) were screened using following criteria: |log2(FoldChange)| > 1 &

851 padj<= 0.05.

852

853 **Preparation of samples for Metabolome sequencing**

854 Metabolome-seq of bacterial was done with four biological replicates that were
855 independently generated, collected, and processed. Total of three group E. coli
856 sample including: *E. coli K12* (Con), HK-*E. coli K12* (HK), and HK-*E. coli yfbR*
857 mutant (HY). All bacteria were overnight cultured to the same OD (OD600=1).
858 *E. coli K12* and *E. coli yfbR* mutant are heat-killed (80, 180min), *E. coli* K12,
859 HK-*E. coli* K12 and HK-*E. coli yfbR* mutant were then spread out NGM plate for
860 72hs at room temperature. Finally, sample was collected into 1.5ml tube by
861 using sterile cell scraping.
862

863 **Metabolome sequencing and data processing**

864 Metabolome were sequenced using the Ultra Performance Liquid
865 Chromatography (UPLC) (ExionLC AD，https://sciex.com.cn/) and Quadrupole-
866 Time of Flight (TripleTOF 6600, AB SCIEX) for Non-targeted; Ultra Performance
867 Liquid Chromatography (UPLC) (ExionLC AD， https://sciex.com.cn/) and
868 Tandem mass spectrometry（MS/MS）（QTRAP®，https://sciex.com/）for Broad
869 targeting (Metware, Wuhan, China). Multiple reaction monitoring (MRM) was
870 used to calculate the expression level of each metabolite. Differential
871 metabolites were screened through Fold change ≥ 2 or Fold change ≤ 0.5 and
872 VIP ≥ 1 (Variable Importance in Projection of OPLS-DA model).
873

874 **Microscopy**

875 Analysis of fluorescence was performed with an Olympus BX53 microscope or
876 Olympus MVX10 dissecting with a DP80 camera.
877

878 **QUANTIFICATION AND STATISTICAL ANALYSIS**

879 **Quantification**

880 ImageJ software was used for quantifying fluorescence intensity of UPR^{ER} and
881 Innate immunity reporter. ImageJ software was used for counting the number
882 of worms about selection and aversion behavior.
883

Statistical analysis

All statistical analyses were preformed using Student's t-test in Graphpad prism 8.0. Two-tailed unpaired t test was used for statistical analysis of two groups of samples. Data are presented as Mean±SD, and $p<0.05$ was considered a significant difference, "*" represents $p<0.05$, "**" represents $p<0.01$, "***" is represents < 0.001, "****" represents $p<0.0001$, "ns" represents no significant difference. For all figures, ''n'' represents the number of worms scored from at least three independent experiments.

Reference:

1. Filosa, A., Barker, A.J., Dal Maschio, M., and Baier, H. (2016). Feeding State Modulates Behavioral Choice and Processing of Prey Stimuli in the Zebrafish Tectum. Neuron *90*, 596-608. 10.1016/j.neuron.2016.03.014.
2. Florsheim, E.B., Sullivan, Z.A., Khoury-Hanold, W., and Medzhitov, R. (2021). Food allergy as a biological food quality control system. Cell *184*, 1440-1454. 10.1016/j.cell.2020.12.007.
3. McLachlan, I.G., Kramer, T.S., Dua, M., DiLoreto, E.M., Gomes, M.A., Dag, U., Srinivasan, J., and Flavell, S.W. (2022). Diverse states and stimuli tune olfactory receptor expression levels to modulate food-seeking behavior. Elife *11*. 10.7554/eLife.79557.
4. Avery, J.A., Liu, A.G., Ingeholm, J.E., Gotts, S.J., and Martin, A. (2021). Viewing images of foods evokes taste quality-specific activity in gustatory insular cortex. Proc Natl Acad Sci U S A *118*. 10.1073/pnas.2010932118.
5. Melin, A.D., Nevo, O., Shirasu, M., Williamson, R.E., Garrett, E.C., Endo, M., Sakurai, K., Matsushita, Y., Touhara, K., and Kawamura, S. (2019). Fruit scent and observer colour vision shape food-selection strategies in wild capuchin monkeys. Nat Commun *10*, 2407. 10.1038/s41467-019-10250-9.
6. Bargmann, C.I. (2006). Chemosensation in C. elegans. WormBook, 1-29. 10.1895/wormbook.1.123.1.
7. Sengupta, P., Chou, J.H., and Bargmann, C.I. (1996). odr-10 encodes a seven transmembrane domain olfactory receptor required for responses to the odorant diacetyl. Cell *84*, 899-909. 10.1016/s0092-8674(00)81068-5.
8. Troemel, E.R., Kimmel, B.E., and Bargmann, C.I. (1997). Reprogramming chemotaxis responses: sensory neurons define olfactory preferences in C. elegans. Cell *91*, 161-169. 10.1016/s0092-8674(00)80399-2.
9. Fiala, A. (2007). Olfaction and olfactory learning in Drosophila: recent progress. Curr Opin Neurobiol *17*, 720-726. 10.1016/j.conb.2007.11.009.
10. Chalasani, S.H., Chronis, N., Tsunozaki, M., Gray, J.M., Ramot, D., Goodman, M.B., and Bargmann, C.I. (2007). Dissecting a circuit for olfactory behaviour in

Caenorhabditis elegans. Nature *450*, 63-70. 10.1038/nature06292.
11. Zhang, B., Jun, H., Wu, J., Liu, J., and Xu, X.Z.S. (2021). Olfactory perception of food abundance regulates dietary restriction-mediated longevity via a brain-to-gut signal. Nat Aging *1*, 255-268. 10.1038/s43587-021-00039-1.
12. Ha, H.I., Hendricks, M., Shen, Y., Gabel, C.V., Fang-Yen, C., Qin, Y., Colon-Ramos, D., Shen, K., Samuel, A.D., and Zhang, Y. (2010). Functional organization of a neural network for aversive olfactory learning in Caenorhabditis elegans. Neuron *68*, 1173-1186. 10.1016/j.neuron.2010.11.025.
13. Scott, K. (2018). Gustatory Processing in Drosophila melanogaster. Annu Rev Entomol *63*, 15-30. 10.1146/annurev-ento-020117-043331.
14. Hukema, R.K., Rademakers, S., Dekkers, M.P., Burghoorn, J., and Jansen, G. (2006). Antagonistic sensory cues generate gustatory plasticity in Caenorhabditis elegans. Embo J *25*, 312-322. 10.1038/sj.emboj.7600940.
15. Ni, L., Bronk, P., Chang, E.C., Lowell, A.M., Flam, J.O., Panzano, V.C., Theobald, D.L., Griffith, L.C., and Garrity, P.A. (2013). A gustatory receptor paralogue controls rapid warmth avoidance in Drosophila. Nature *500*, 580-584. 10.1038/nature12390.
16. Jones, D., and Candido, E.P.M. (1999). Feeding is inhibited by sublethal concentrations of toxicants and by heat stress in the nematode Caenorhabditis elegans: Relationship to the cellular stress response. J Exp Zool *284*, 147-157. Doi 10.1002/(Sici)1097-010x(19990701)284:2<147::Aid-Jez4>3.3.Co;2-Q.
17. Xie, Z., Zhang, X., Zhao, M., Huo, L., Huang, M., Li, D., Zhang, S., Cheng, X., Gu, H., Zhang, C., et al. (2022). The gut-to-brain axis for toxin-induced defensive responses. Cell *185*, 4298-4316 e4221. 10.1016/j.cell.2022.10.001.
18. Richardson, C.E., Kooistra, T., and Kim, D.H. (2010). An essential role for XBP-1 in host protection against immune activation in C. elegans. Nature *463*, 1092-U1114. 10.1038/nature08762.
19. Kim, D.H., Feinbaum, R., Alloing, G., Emerson, F.E., Garsin, D.A., Inoue, H., Tanaka-Hino, M., Hisamoto, N., Matsumoto, K., Tan, M.W., and Ausubel, F.M. (2002). A conserved p38 MAP kinase pathway in Caenorhabditis elegans innate immunity. Science *297*, 623-626. 10.1126/science.1073759.
20. Carr, A.C., and Maggini, S. (2017). Vitamin C and Immune Function. Nutrients *9*. 10.3390/nu9111211.
21. Steinert, R.E., Lee, Y.K., and Sybesma, W. (2020). Vitamins for the Gut Microbiome. Trends Mol Med *26*, 137-140. 10.1016/j.molmed.2019.11.005.
22. Li, Y., and Schellhorn, H.E. (2007). New developments and novel therapeutic perspectives for vitamin C. J Nutr *137*, 2171-2184. 10.1093/jn/137.10.2171.
23. Carr, A.C., and Frei, B. (1999). Toward a new recommended dietary allowance for vitamin C based on antioxidant and health effects in humans. Am J Clin Nutr *69*, 1086-1107. 10.1093/ajcn/69.6.1086.
24. Qi, B., Kniazeva, M., and Han, M. (2017). A vitamin-B2-sensing mechanism that regulates gut protease activity to impact animal's food behavior and

growth. Elife *6*. 10.7554/eLife.26243.
25. Qi, B., and Han, M. (2018). Microbial Siderophore Enterobactin Promotes Mitochondrial Iron Uptake and Development of the Host via Interaction with ATP Synthase. Cell *175*, 571-582.e511. 10.1016/j.cell.2018.07.032.
26. Nakad, R., Snoek, L.B., Yang, W., Ellendt, S., Schneider, F., Mohr, T.G., Rösingh, L., Masche, A.C., Rosenstiel, P.C., Dierking, K., et al. (2016). Contrasting invertebrate immune defense behaviors caused by a single gene, the Caenorhabditis elegans neuropeptide receptor gene npr-1. BMC Genomics *17*, 280. 10.1186/s12864-016-2603-8.
27. Sinha, A., Rae, R., Iatsenko, I., and Sommer, R.J. (2012). System wide analysis of the evolution of innate immunity in the nematode model species Caenorhabditis elegans and Pristionchus pacificus. PLoS One *7*, e44255. 10.1371/journal.pone.0044255.
28. Hetz, C., Zhang, K., and Kaufman, R.J. (2020). Mechanisms, regulation and functions of the unfolded protein response. Nat Rev Mol Cell Biol *21*, 421-438. 10.1038/s41580-020-0250-z.
29. Ron, D., and Walter, P. (2007). Signal integration in the endoplasmic reticulum unfolded protein response. Nat Rev Mol Cell Biol *8*, 519-529. 10.1038/nrm2199.
30. Fletcher, M., Tillman, E.J., Butty, V.L., Levine, S.S., and Kim, D.H. (2019). Global transcriptional regulation of innate immunity by ATF-7 in C. elegans. Plos Genet *15*. ARTN e1007830
10.1371/journal.pgen.1007830.
31. Foster, K.J., McEwan, D.L., and Pukkila-Worley, R. (2020). Measurements of Innate Immune Function in C. elegans. Methods Mol Biol *2144*, 145-160. 10.1007/978-1-0716-0592-9_13.
32. Weiss, B. (2007). The Deoxycytidine Pathway for Thymidylate Synthesis in Escherichia coli. Journal of Bacteriology *189*, 7922-7926. 10.1128/jb.00461-07.
33. Franceus, J., and Desmet, T. (2020). Sucrose Phosphorylase and Related Enzymes in Glycoside Hydrolase Family 13: Discovery, Application and Engineering. International Journal of Molecular Sciences *21*. 10.3390/ijms21072526.
34. Xing, S., Zhang, L., Lin, H., Mao, Z., Bao, K., Hao, P., Pei, Z., Li, J., and Hu, Z. (2019). Lactose induced redox-dependent senescence and activated Nrf2 pathway. Int J Clin Exp Pathol *12*, 2034-2045.
35. Patananan, A.N., Budenholzer, L.M., Pedraza, M.E., Torres, E.R., Adler, L.N., and Clarke, S.G. (2015). The invertebrate Caenorhabditis elegans biosynthesizes ascorbate. Arch Biochem Biophys *569*, 32-44. 10.1016/j.abb.2015.02.002.
36. Yabuta, Y., Nagata, R., Aoki, Y., Kariya, A., Wada, K., Yanagimoto, A., Hara, H., Bito, T., Okamoto, N., Yoshida, S., et al. (2020). L-Ascorbate Biosynthesis Involves Carbon Skeleton Rearrangement in the Nematode Caenorhabditis elegans. Metabolites *10*. 10.3390/metabo10080334.
37. Moritz, B., Schmitz, A.E., Rodrigues, A.L.S., Dafre, A.L., and Cunha, M.P.

1011 (2020). The role of vitamin C in stress-related disorders. The Journal of
1012 Nutritional Biochemistry *85*. 10.1016/j.jnutbio.2020.108459.
1013 38. Rice, M.E. (2000). Ascorbate regulation and its neuroprotective role in the
1014 brain. Trends in Neurosciences *23*, 209-216. https://doi.org/10.1016/S0166-
1015 2236(99)01543-X.
1016 39. Webb, A.L., and Villamor, E. (2007). Update: Effects of Antioxidant and Non-
1017 Antioxidant Vitamin Supplementation on Immune Function. Nutrition
1018 Reviews *65*, 181-217. 10.1111/j.1753-4887.2007.tb00298.x.
1019 40. Maggini, S., Wintergerst, E.S., Beveridge, S., and Hornig, D.H. (2007). Selected
1020 vitamins and trace elements support immune function by strengthening
1021 epithelial barriers and cellular and humoral immune responses. British
1022 Journal of Nutrition *98*, S29-S35. 10.1017/s0007114507832971.
1023 41. Luo, X., Ng, C., He, J., Yang, M., Luo, X., Herbert, T.P., and Whitehead, J.P.
1024 (2022). Vitamin C protects against hypoxia, inflammation, and ER stress in
1025 primary human preadipocytes and adipocytes. Molecular and Cellular
1026 Endocrinology *556*. 10.1016/j.mce.2022.111740.
1027 42. Su, M., Liang, X., Xu, X., Wu, X., and Yang, B. (2019). Hepatoprotective
1028 benefits of vitamin C against perfluorooctane sulfonate-induced liver damage
1029 in mice through suppressing inflammatory reaction and ER stress.
1030 Environmental Toxicology and Pharmacology *65*, 60-65.
1031 10.1016/j.etap.2018.12.004.
1032 43. Ozbey, N.P., Thompson, M.A., and Taylor, R.C. (2021). The regulation of animal
1033 behavior by cellular stress responses. Exp Cell Res *405*, 112720.
1034 10.1016/j.yexcr.2021.112720.
1035 44. Ozbey, N.P., Imanikia, S., Krueger, C., Hardege, I., Morud, J., Sheng, M.,
1036 Schafer, W.R., Casanueva, M.O., and Taylor, R.C. (2020). Tyramine Acts
1037 Downstream of Neuronal XBP-1s to Coordinate Inter-tissue UPR(ER)
1038 Activation and Behavior in C. elegans. Dev Cell *55*, 754-770 e756.
1039 10.1016/j.devcel.2020.10.024.
1040 45. Troemel, E.R., Chu, S.W., Reinke, V., Lee, S.S., Ausubel, F.M., and Kim, D.H.
1041 (2006). p38 MAPK regulates expression of immune response genes and
1042 contributes to longevity in C. elegans. Plos Genet *2*, e183.
1043 10.1371/journal.pgen.0020183.
1044 46. Mouysset, J., Kahler, C., and Hoppe, T. (2006). A conserved role of
1045 Caenorhabditis elegans CDC-48 in ER-associated protein degradation. J Struct
1046 Biol *156*, 41-49. 10.1016/j.jsb.2006.02.015.
1047 47. Sasagawa, Y., Otani, M., Higashitani, N., Higashitani, A., Sato, K., Ogura, T., and
1048 Yamanaka, K. (2009). Caenorhabditis elegans p97 controls germline-specific
1049 sex determination by controlling the TRA-1 level in a CUL-2-dependent
1050 manner. Journal of Cell Science *122*, 3663-3672. 10.1242/jcs.052415.
1051 48. Kim, K., and Li, C. (2004). Expression and regulation of an FMRFamide-related
1052 neuropeptide gene family in Caenorhabditis elegans. J Comp Neurol *475*, 540-
1053 550. 10.1002/cne.20189.
1054 49. Melo, J.A., and Ruvkun, G. (2012). Inactivation of conserved C. elegans genes

1055 engages pathogen- and xenobiotic-associated defenses. Cell *149*, 452-466.
1056 10.1016/j.cell.2012.02.050.
1057 50. Geng, S., Li, Q., Zhou, X., Zheng, J., Liu, H., Zeng, J., Yang, R., Fu, H., Hao, F.,
1058 Feng, Q., and Qi, B. (2022). Gut commensal E. coli outer membrane proteins
1059 activate the host food digestive system through neural-immune
1060 communication. Cell Host Microbe. 10.1016/j.chom.2022.08.004.
1061 51. Richardson, C.E., Kinkel, S., and Kim, D.H. (2011). Physiological IRE-1-XBP-1
1062 and PEK-1 signaling in Caenorhabditis elegans larval development and
1063 immunity. PLoS Genet *7*, e1002391. 10.1371/journal.pgen.1002391.
1064 52. Kamath, R.S., Fraser, A.G., Dong, Y., Poulin, G., Durbin, R., Gotta, M., Kanapin,
1065 A., Le Bot, N., Moreno, S., Sohrmann, M., et al. (2003). Systematic functional
1066 analysis of the Caenorhabditis elegans genome using RNAi. Nature *421*, 231-
1067 237. 10.1038/nature01278.
1068 53. Rual, J.F., Ceron, J., Koreth, J., Hao, T., Nicot, A.S., Hirozane-Kishikawa, T.,
1069 Vandenhaute, J., Orkin, S.H., Hill, D.E., van den Heuvel, S., and Vidal, M.
1070 (2004). Toward improving Caenorhabditis elegans phenome mapping with an
1071 ORFeome-based RNAi library. Genome Res *14*, 2162-2168.
1072 10.1101/gr.2505604.
1073 54. Mortazavi, A., Williams, B.A., McCue, K., Schaeffer, L., and Wold, B. (2008).
1074 Mapping and quantifying mammalian transcriptomes by RNA-Seq. Nat
1075 Methods *5*, 621-628. 10.1038/nmeth.1226.
1076 55. Liao, Y., Smyth, G.K., and Shi, W. (2014). featureCounts: an efficient general
1077 purpose program for assigning sequence reads to genomic features.
1078 Bioinformatics *30*, 923-930. 10.1093/bioinformatics/btt656.
1079 56. Love, M.I., Huber, W., and Anders, S. (2014). Moderated estimation of fold
1080 change and dispersion for RNA-seq data with DESeq2. Genome Biol *15*. ARTN
1081 550
1082 10.1186/s13059-014-0550-8.
1083

Figure 1

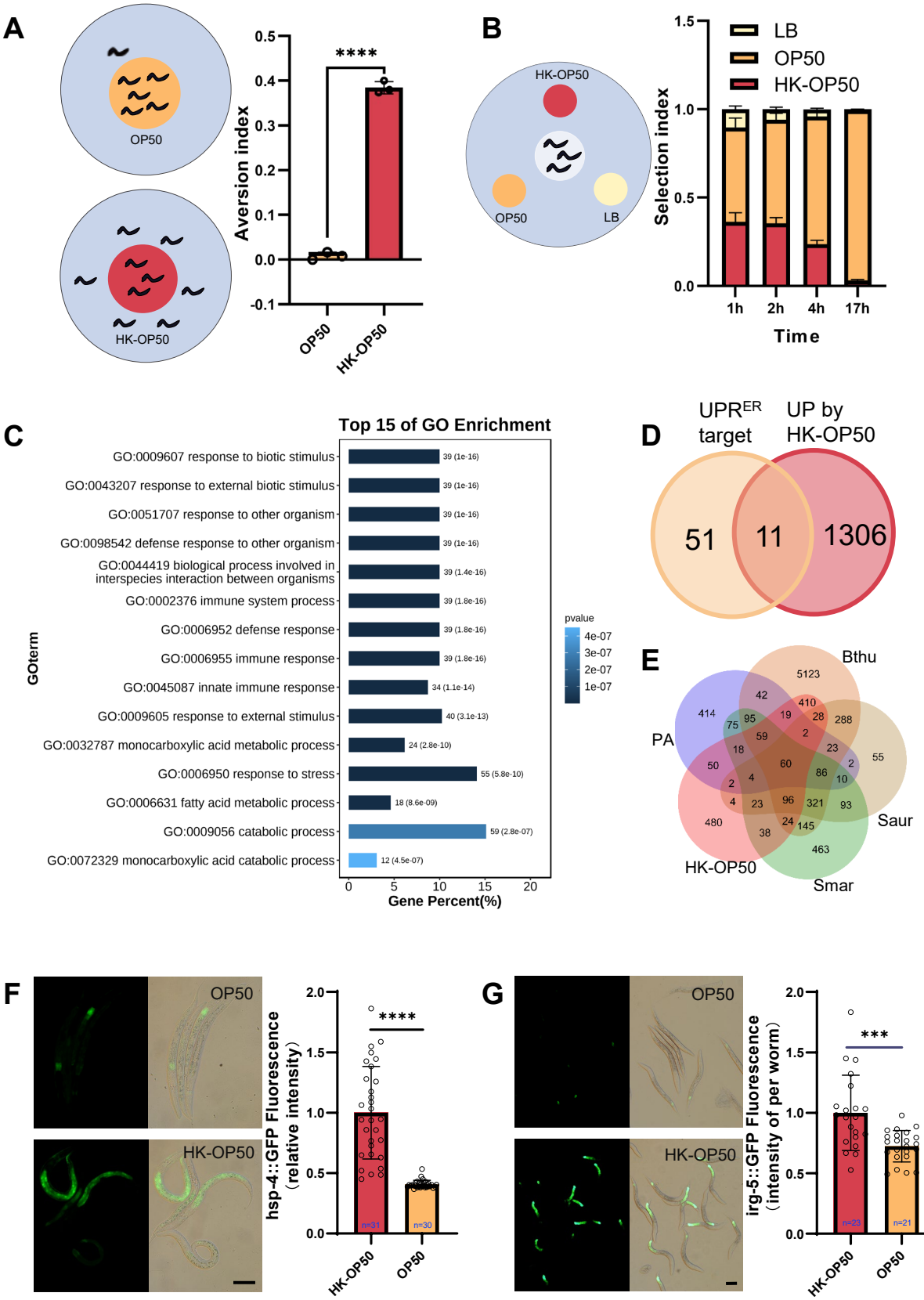
A
OP50
HK-OP50
Aversion index
****
OP50
HK-OP50
B
HK-OP50
OP50
LB
Selection index
LB
OP50
HK-OP50
1h
2h
4h
17h
Time
C
Top 15 of GO Enrichment
GOterm
GO:0009607 response to biotic stimulus
GO:0043207 response to external biotic stimulus
GO:0051707 response to other organism
GO:0098542 defense response to other organism
GO:0044419 biological process involved in interspecies interaction between organisms
GO:0002376 immune system process
GO:0006952 defense response
GO:0006955 immune response
GO:0045087 innate immune response
GO:0009605 response to external stimulus
GO:0032787 monocarboxylic acid metabolic process
GO:0006950 response to stress
GO:0006631 fatty acid metabolic process
GO:0009056 catabolic process
GO:0072329 monocarboxylic acid catabolic process
39 (1e-16)
39 (1e-16)
39 (1e-16)
39 (1e-16)
39 (1.4e-16)
39 (1.8e-16)
39 (1.8e-16)
39 (1.8e-16)
34 (1.1e-14)
40 (3.1e-13)
24 (2.8e-10)
55 (5.8e-10)
18 (8.6e-09)
59 (2.8e-07)
12 (4.5e-07)
Gene Percent(%)
pvalue
4e-07
3e-07
2e-07
1e-07
D
UPR^ER target
UP by HK-OP50
51
11
1306
E
Bthu
PA
Saur
HK-OP50
Smar
F
OP50
HK-OP50
hsp-4::GFP Fluorescence (relative intensity)
****
n=31
n=30
HK-OP50
OP50
G
OP50
HK-OP50
irg-5::GFP Fluorescence (intensity of per worm)
***
n=23
n=21
HK-OP50
OP50

Figure 2

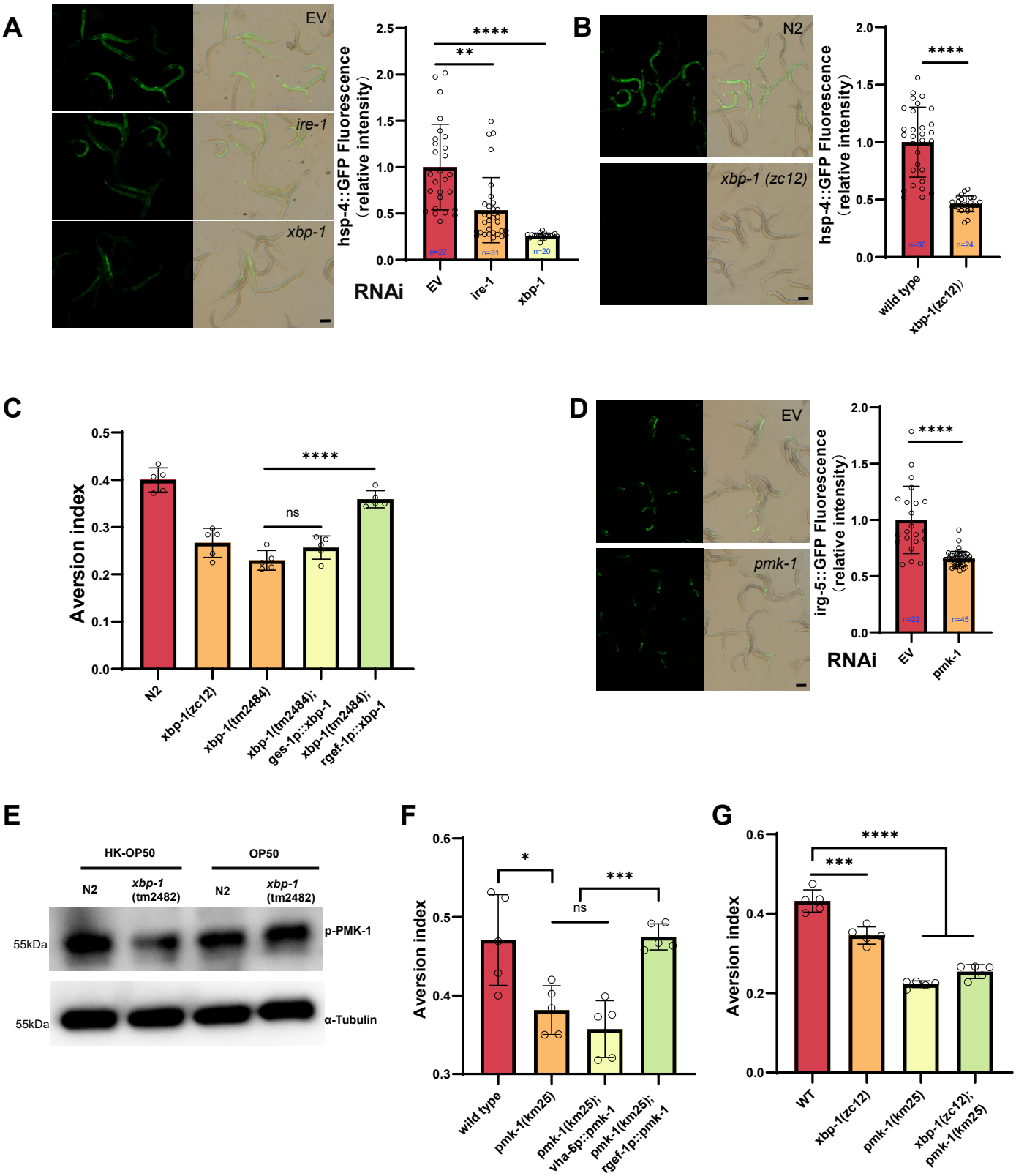
A
EV
ire-1
xbp-1
hsp-4::GFP Fluorescence (relative intensity)
****
**
n=27
n=31
n=20
RNAi
EV
ire-1
xbp-1
B
N2
xbp-1 (zc12)
hsp-4::GFP Fluorescence (relative intensity)
****
n=30
n=24
wild type
xbp-1(zc12))
C
Aversion index
****
ns
N2
xbp-1(zc12)
xbp-1(tm2484)
xbp-1(tm2484); ges-1p::xbp-1
xbp-1(tm2484); rgef-1p::xbp-1
D
EV
pmk-1
irg-5::GFP Fluorescence (relative intensity)
****
n=22
n=45
RNAi
EV
pmk-1
E
HK-OP50
OP50
N2
xbp-1 (tm2482)
N2
xbp-1 (tm2482)
55kDa
p-PMK-1
55kDa
α-Tubulin
F
Aversion index
*
***
ns
wild type
pmk-1(km25)
pmk-1(km25); vha-6p::pmk-1
pmk-1(km25); rgef-1p::pmk-1
G
Aversion index
****
***
WT
xbp-1(zc12)
pmk-1(km25)
xbp-1(zc12); pmk-1(km25)

Figure 3

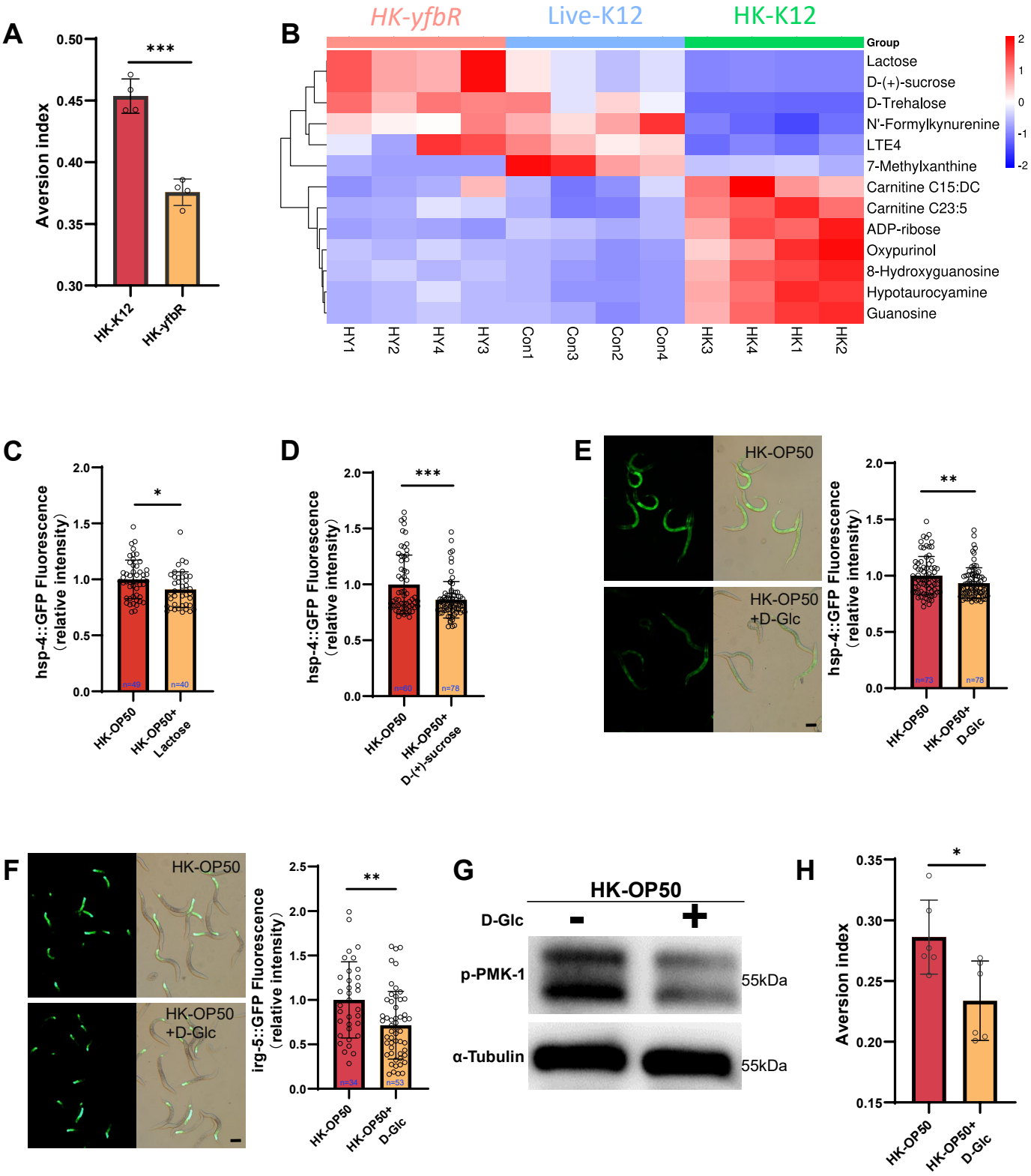
A
Aversion index
0.50
0.45
0.40
0.35
0.30
***
HK-K12
HK-yfbR
B
HK-yfbR
Live-K12
HK-K12
Group
Lactose
D-(+)-sucrose
D-Trehalose
N'-Formylkynurenine
LTE4
7-Methylxanthine
Carnitine C15:DC
Carnitine C23:5
ADP-ribose
Oxypurinol
8-Hydroxyguanosine
Hypotaurocyamine
Guanosine
HY1
HY2
HY4
HY3
Con1
Con3
Con2
Con4
HK3
HK4
HK1
HK2
2
1
0
-1
-2
C
hsp-4::GFP Fluorescence
(relative intensity)
2.0
1.5
1.0
0.5
0.0
*
n=40
n=40
HK-OP50
HK-OP50+
Lactose
D
hsp-4::GFP Fluorescence
(relative intensity)
2.0
1.5
1.0
0.5
0.0
***
n=60
n=78
HK-OP50
HK-OP50+
D-(+)-sucrose
E
HK-OP50
HK-OP50
+D-Glc
hsp-4::GFP Fluorescence
(relative intensity)
2.0
1.5
1.0
0.5
0.0
**
n=73
n=78
HK-OP50
HK-OP50+
D-Glc
F
HK-OP50
HK-OP50
+D-Glc
irg-5::GFP Fluorescence
(relative intensity)
2.5
2.0
1.5
1.0
0.5
0.0
**
n=34
n=53
HK-OP50
HK-OP50+
D-Glc
G
HK-OP50
D-Glc
-
+
p-PMK-1
55kDa
α-Tubulin
55kDa
H
Aversion index
0.35
0.30
0.25
0.20
0.15
*
HK-OP50
HK-OP50+
D-Glc

Figure 4

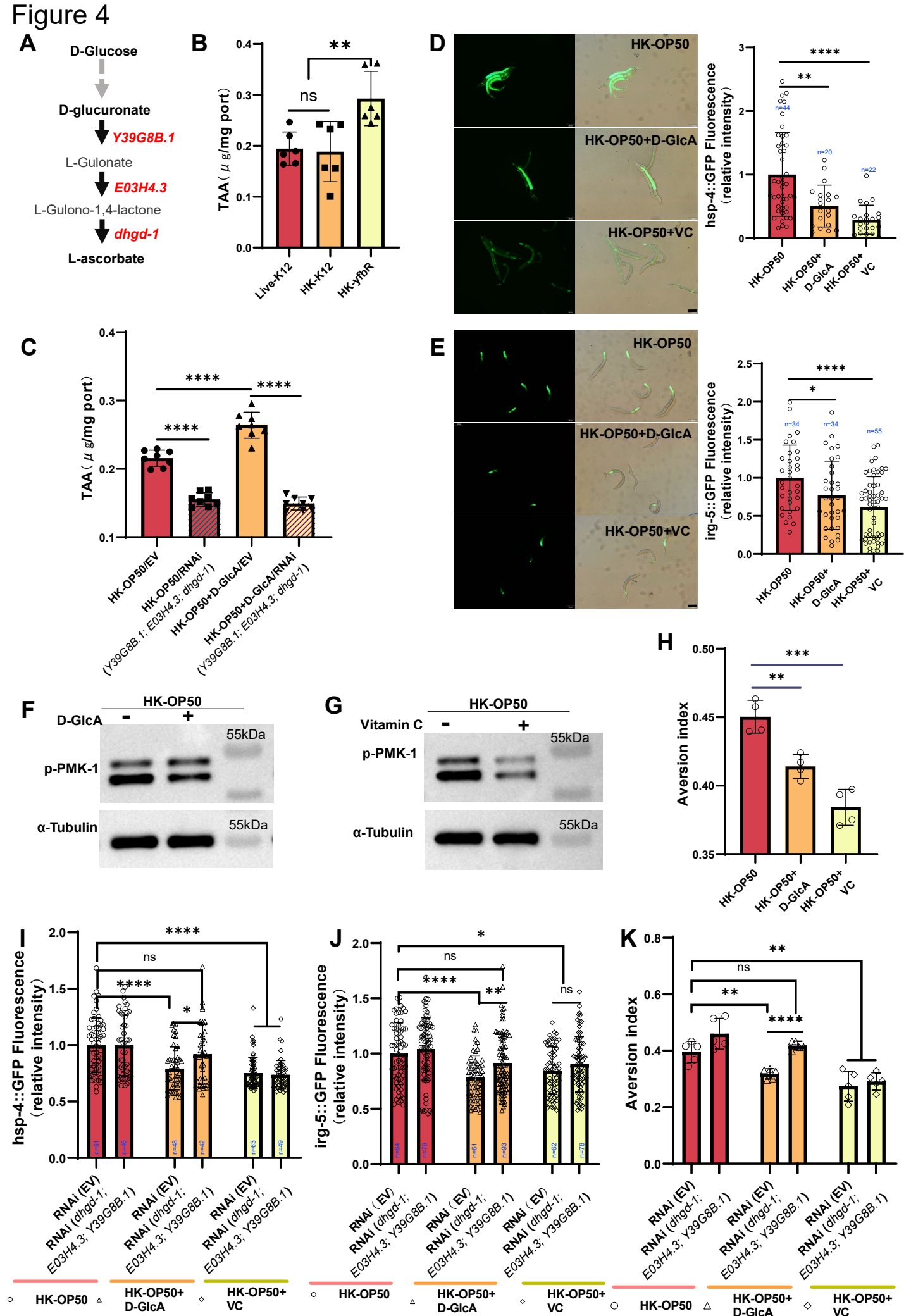
A
D-Glucose
D-glucuronate
Y39G8B.1
L-Gulonate
E03H4.3
L-Gulono-1,4-lactone
dhgd-1
L-ascorbate
B
TAA（μg/mg port）
ns
**
Live-K12
HK-K12
HK-yfbR
C
TAA（μg/mg port）
****
HK-OP50/EV
HK-OP50/RNAi (Y39G8B.1; E03H4.3; dhgd-1)
HK-OP50+D-GlcA/EV
HK-OP50+D-GlcA/RNAi (Y39G8B.1; E03H4.3; dhgd-1)
D
HK-OP50
HK-OP50+D-GlcA
HK-OP50+VC
hsp-4::GFP Fluorescence (relative intensity)
****
**
n=44
n=20
n=22
E
irg-5::GFP Fluorescence (relative intensity)
****
*
n=34
n=34
n=55
F
HK-OP50
D-GlcA
-
+
p-PMK-1
α-Tubulin
55kDa
G
HK-OP50
Vitamin C
-
+
p-PMK-1
α-Tubulin
55kDa
H
Aversion index
***
**
I
hsp-4::GFP Fluorescence (relative intensity)
****
ns
*
J
irg-5::GFP Fluorescence (relative intensity)
*
ns
**
K
Aversion index
**
ns
****
RNAi (EV)
RNAi (dhgd-1; E03H4.3; Y39G8B.1)
HK-OP50
HK-OP50+ D-GlcA
HK-OP50+ VC

Figure 5

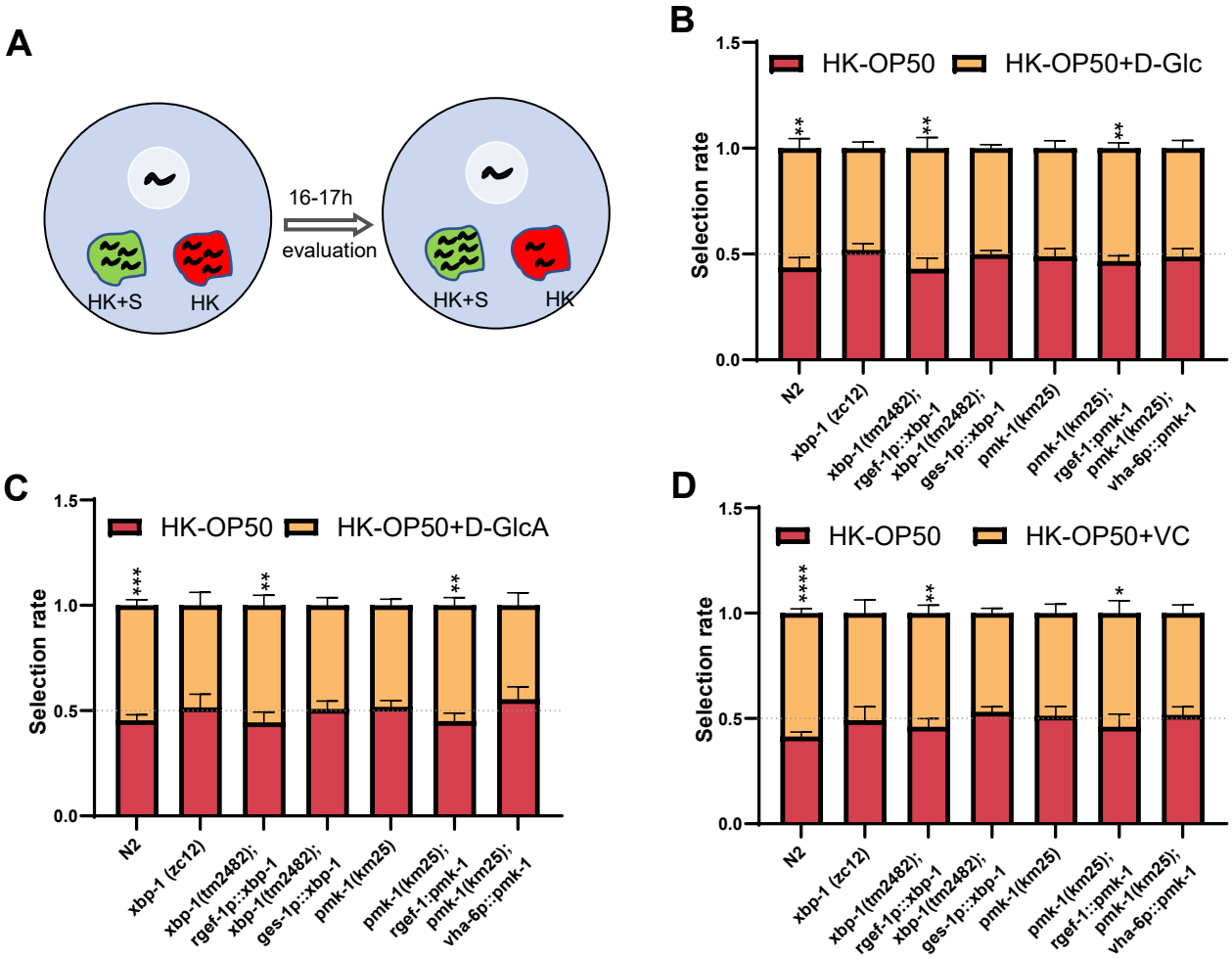
A
HK+S
HK
16-17h
evaluation
HK+S
HK
B
HK-OP50
HK-OP50+D-Glc
Selection rate
1.5
1.0
0.5
0.0
**
**
**
N2
xbp-1 (zc12)
xbp-1(tm2482);
rgef-1p::xbp-1
xbp-1(tm2482);
ges-1p::xbp-1
pmk-1(km25)
pmk-1(km25);
rgef-1::pmk-1
pmk-1(km25);
vha-6p::pmk-1
C
HK-OP50
HK-OP50+D-GlcA
Selection rate
1.5
1.0
0.5
0.0
***
**
**
N2
xbp-1 (zc12)
xbp-1(tm2482);
rgef-1p::xbp-1
xbp-1(tm2482);
ges-1p::xbp-1
pmk-1(km25)
pmk-1(km25);
rgef-1::pmk-1
pmk-1(km25);
vha-6p::pmk-1
D
HK-OP50
HK-OP50+VC
Selection rate
1.5
1.0
0.5
0.0
****
**
*
N2
xbp-1 (zc12)
xbp-1(tm2482);
rgef-1p::xbp-1
xbp-1(tm2482);
ges-1p::xbp-1
pmk-1(km25)
pmk-1(km25);
rgef-1::pmk-1
pmk-1(km25);
vha-6p::pmk-1

Figure 6

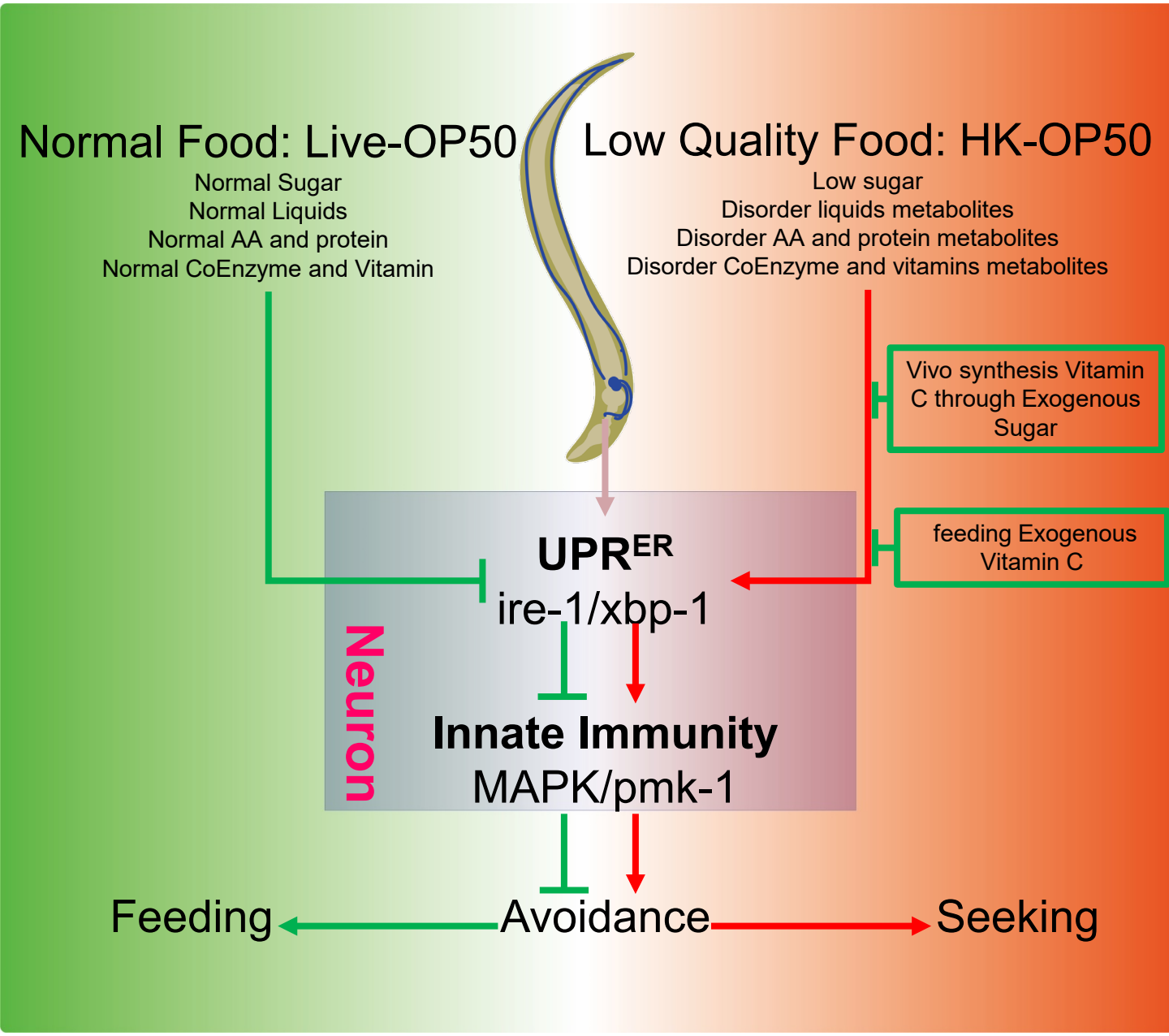
Normal Food: Live-OP50
Normal Sugar
Normal Liquids
Normal AA and protein
Normal CoEnzyme and Vitamin
Low Quality Food: HK-OP50
Low sugar
Disorder liquids metabolites
Disorder AA and protein metabolites
Disorder CoEnzyme and vitamins metabolites
Vivo synthesis Vitamin C through Exogenous Sugar
feeding Exogenous Vitamin C
UPR^ER
ire-1/xbp-1
Neuron
Innate Immunity
MAPK/pmk-1
Feeding
Avoidance
Seeking

Figure S1

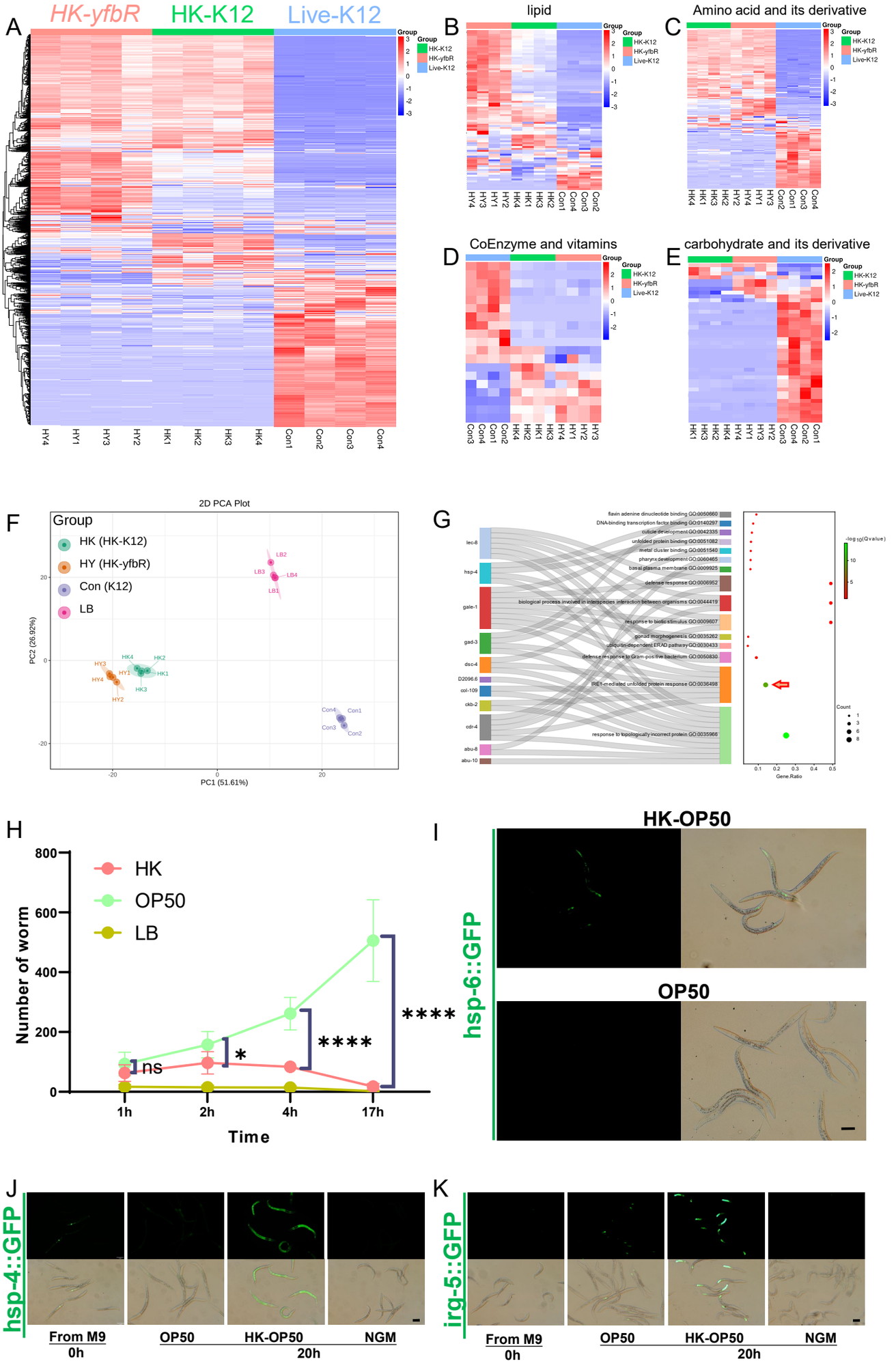
A
HK-yfbR
HK-K12
Live-K12
Group
HK-K12
HK-yfbR
Live-K12
HY4 HY1 HY3 HY2 HK1 HK2 HK3 HK4 Con1 Con2 Con3 Con4
B
lipid
C
Amino acid and its derivative
D
CoEnzyme and vitamins
E
carbohydrate and its derivative
F
2D PCA Plot
Group
HK (HK-K12)
HY (HK-yfbR)
Con (K12)
LB
PC1 (51.61%)
PC2 (26.92%)
G
H
HK
OP50
LB
Number of worm
Time
1h
2h
4h
17h
ns
*
****
****
I
HK-OP50
OP50
hsp-6::GFP
J
hsp-4::GFP
From M9
0h
OP50
HK-OP50
NGM
20h
K
irg-5::GFP
From M9
0h
OP50
HK-OP50
NGM
20h

Figure S1. Food selection assay of animals fed HK-*E. coli* or *E. coli.* Relative to Figure 1.

(A-E) Metabolomics analysis of different quality food (HK-K12, HK-*yfbR* and Live-K12). Cluster analysis of all metabolites (A), lipids and their derivatives (B), amino acids and their derivatives (C), coenzymes and vitamins (D), and carbohydrates and their derivatives (E) from Live-K12, HK-K12, and HK-yfbR. Color indicates the relative level of each metabolite. HK-K12: heat-killed *E. coli* wild-type K12; HK-*yfbR:* heat-killed *E. coli mutant yfbR;* K12: live *E. coli* wild-type K12. z-score for standardizing data, complete for bi-clustering algorithm, and Euclidean for distance method.

(A) Principal component analysis to test the repeatability of the metabolic experiment. HK-K12: heat-killed *E. coli* wild-type K12; HK-yfbR: heat-killed *E. coli* mutant yfbR; K12: live *E. coli* wild-type K12. LB: LB buffer for culturing *E. coli.*

(B) GO enrichment analysis of UPR^{ER} dependent IRE-1 branch.

(C) The number of worms in each position calculated at the indicated time, indicating that animals initially select both foods (1-2h), but eventually favor high-quality food (Live E. coli) until 17h.

(D) UPR^{mit} Reporter (*Phsp-6:GFP*) was weakly induced in animals fed with HK-E. coli

(E) UPR^{ER} Reporter (Phsp-4:GFP) expression in animals under normal food (OP50), low quality food (HK-OP50), and starved (M9: hatching L1 worm in M9, NGM) condition;

(F) Immunity Reporter (Pirg-5:GFP) expression in animals under normal food (OP50), low quality food (HK-OP50), and starved (M9: hatching L1 worm in M9, NGM).

For all panels, Scale bar shows on indicated figures, 50 μm. * $p<0.05$, ** $p<0.01$, *** $p < 0.001$, **** $p<0.0001$, ns: no significant difference. Precise P values are provided in Raw Data.

Figure S2

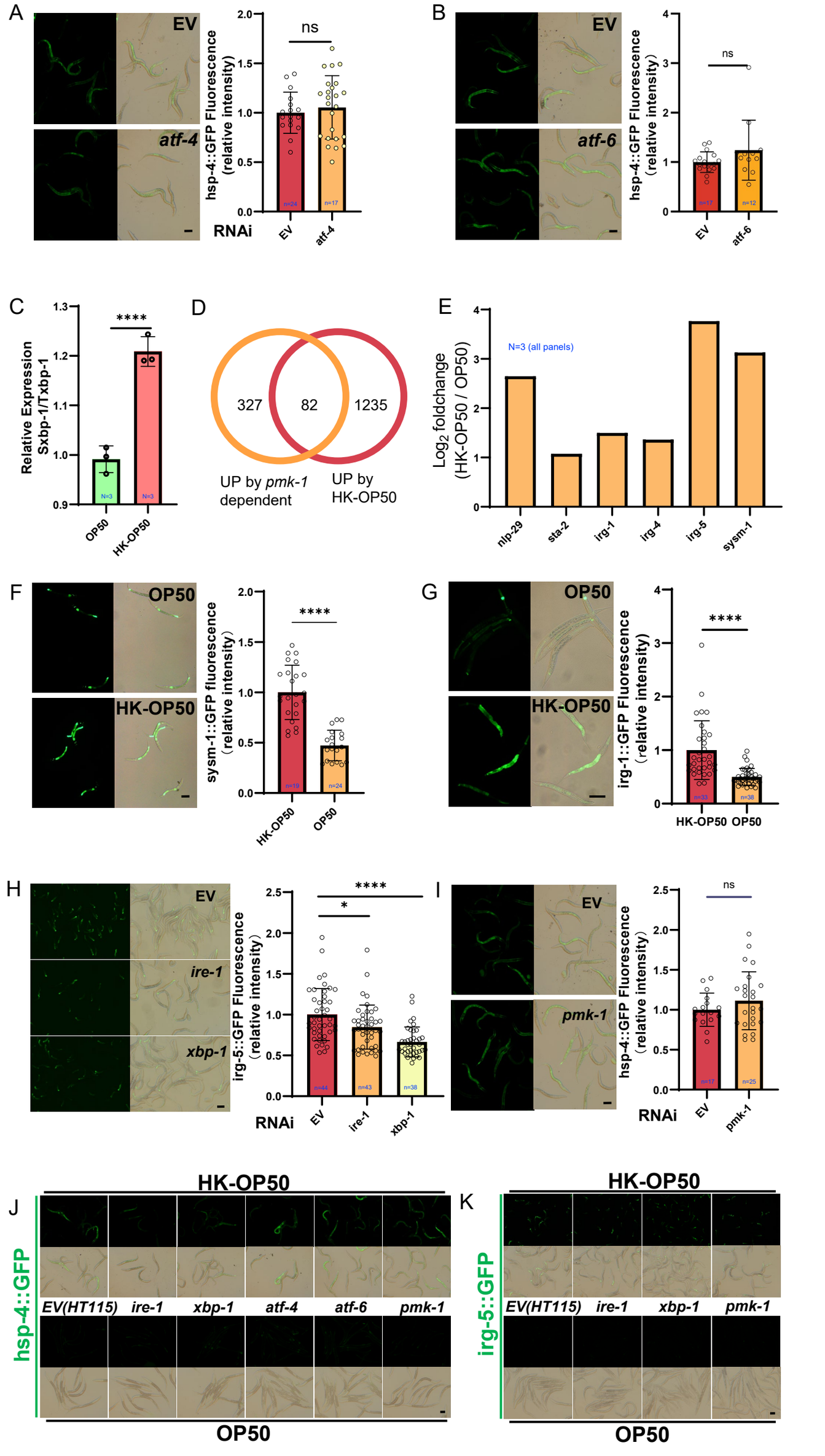
A
EV
atf-4
hsp-4::GFP Fluorescence (relative intensity)
ns
RNAi
EV
atf-4
B
EV
atf-6
hsp-4::GFP Fluorescence (relative intensity)
ns
EV
atf-6
C
Relative Expression Sxbp-1/Txbp-1
****
OP50
HK-OP50
D
327
82
1235
UP by pmk-1 dependent
UP by HK-OP50
E
Log2 foldchange (HK-OP50 / OP50)
N=3 (all panels)
nlp-29
sta-2
irg-1
irg-4
irg-5
sysm-1
F
OP50
HK-OP50
sysm-1::GFP fluorescence (relative intensity)
****
HK-OP50
OP50
G
OP50
HK-OP50
irg-1::GFP Fluorescence (relative intensity)
****
HK-OP50
OP50
H
EV
ire-1
xbp-1
irg-5::GFP Fluorescence (relative intensity)
****
*
RNAi
EV
ire-1
xbp-1
I
EV
pmk-1
hsp-4::GFP Fluorescence (relative intensity)
ns
RNAi
EV
pmk-1
J
HK-OP50
hsp-4::GFP
EV(HT115)
ire-1
xbp-1
atf-4
atf-6
pmk-1
OP50
K
HK-OP50
irg-5::GFP
EV(HT115)
ire-1
xbp-1
pmk-1
OP50

Figure S2. UPRER and Innate immunity pathway in animals are critical for evaluating HK-*E. coli*. Relative to Figure 2.

(A-B) GFP fluorescence images and bar graph showing that HK-*E. coli* induced *Phsp-4::GFP* was not affected in animals with *atf-4* (A) or *atf-6* (B) RNAi treatment. n is the number of worms scored from at least three independent experiments. Data are represented as mean ± SD.

(C) qPCR showing that IRE-1-mediated splicing of *xbp-1* mRNA is induced in animals fed with *HK-E. coli.*

(D) Venn diagram showing the numbers of PMK-1 dependent genes [30] and up-regulated genes in animals fed HK-*E. coli,* and their overlap.

(E) The expression of PMK-1 dependent genes which was extracted from RNA-seq data from animals fed with *HK-E. coli*. The data from average of three independent experiments (N=3)

(F-G) GFP fluorescence images and bar graph showing that *Psysm-1::GFP* (F) and *Pirg-1::GFP* (G) were induced in animals fed *HK-E. coli.* n is the number of worms scored from at least three independent experiments. Data are represented as mean ± SD.

(H) GFP fluorescence images and bar graph showing that HK-*E. coli* induced *Pirg-5::GFP* was decreased in animals with *ire-1* or *xbp-1* RNAi treatment. n is the number of worms scored from at least three independent experiments. Data are represented as mean ± SD.

(I) GFP fluorescence images and bar graph showing that *Phsp-4::GFP* was not affected in animals with *pmk-1* RNAi treatment. n is the number of worms scored from at least three independent experiments. Data are represented as mean ± SD.

(J) UPR^{ER} Reporter (Phsp-4::GFP) expression in animals with candidate RNAi feeding OP50 or HK-OP50

(K) immunity Reporter (Pirg-5::GFP) expression in animals with candidate RNAi feeding OP50 or HK-OP50

For all panels, Scale bar shows on indicated figures, 50 μm. * $p<0.05$, ** $p<0.01$, *** $p < 0.001$, **** $p<0.0001$, ns: no significant difference. Precise P values are provided in Raw Data.

Figure S3

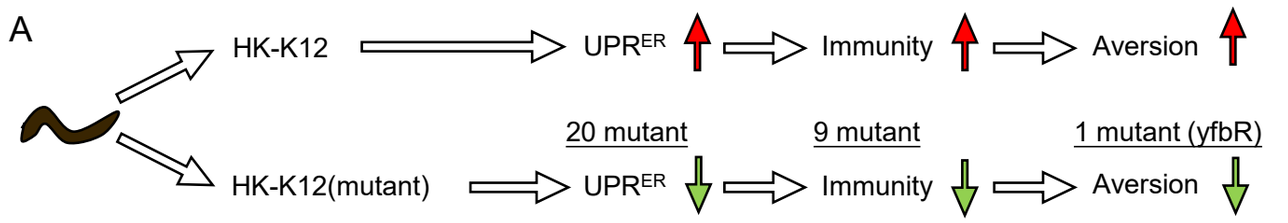
A
HK-K12
UPR^ER
Immunity
Aversion
20 mutant
9 mutant
1 mutant (yfbR)
HK-K12(mutant)
UPR^ER
Immunity
Aversion

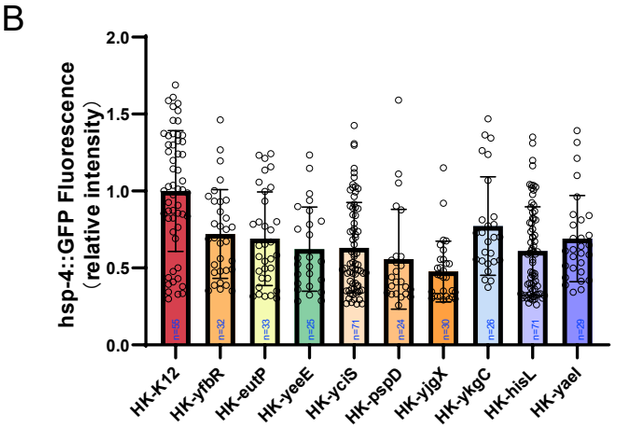
B
hsp-4::GFP Fluorescence
(relative intensity)
HK-K12
HK-yfbR
HK-eutP
HK-yeeE
HK-yciS
HK-pspD
HK-yjgX
HK-ykgC
HK-hisL
HK-yaeI

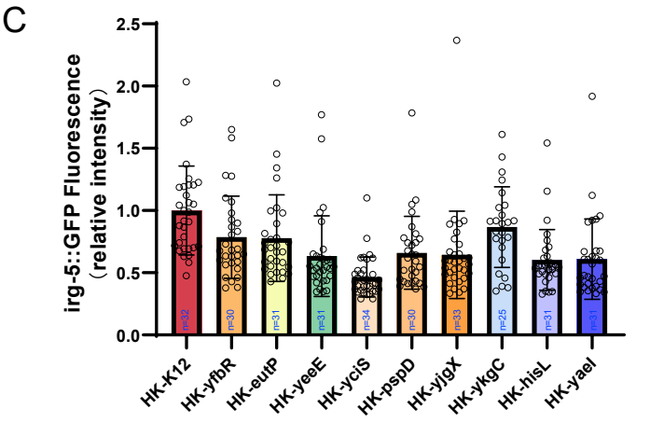
C
irg-5::GFP Fluorescence
(relative intensity)
HK-K12
HK-yfbR
HK-eutP
HK-yeeE
HK-yciS
HK-pspD
HK-yjgX
HK-ykgC
HK-hisL
HK-yaeI

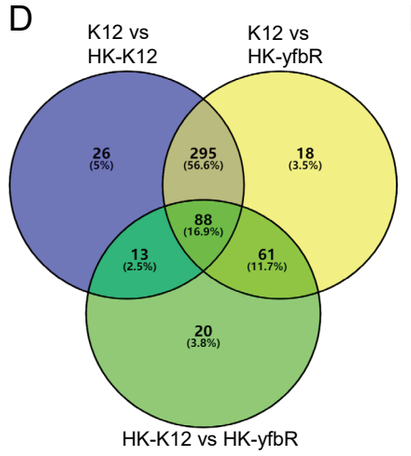
D
K12 vs
HK-K12
K12 vs
HK-yfbR
26
(5%)
295
(56.6%)
18
(3.5%)
88
(16.9%)
13
(2.5%)
61
(11.7%)
20
(3.8%)
HK-K12 vs HK-yfbR

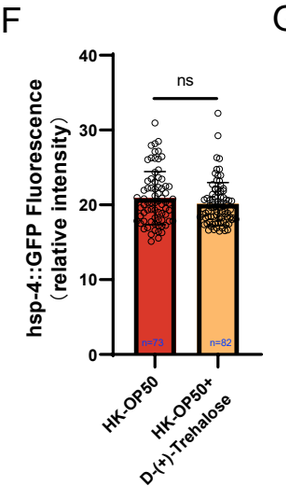
F
ns
hsp-4::GFP Fluorescence
(relative intensity)
HK-OP50
HK-OP50+
D-(+)-Trehalose

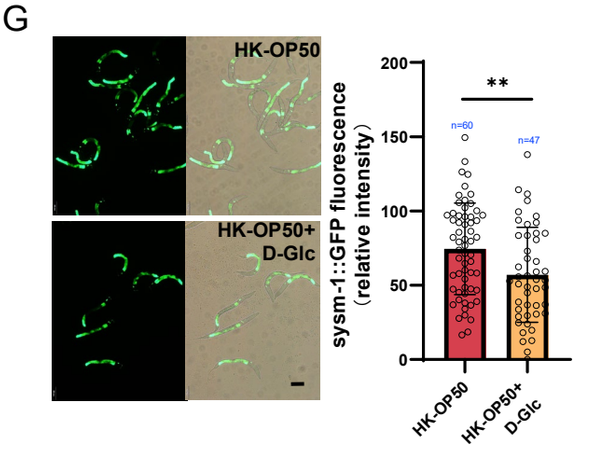
G
HK-OP50
HK-OP50+
D-Glc
**
sysm-1::GFP fluorescence
(relative intensity)
HK-OP50
HK-OP50+
D-Glc

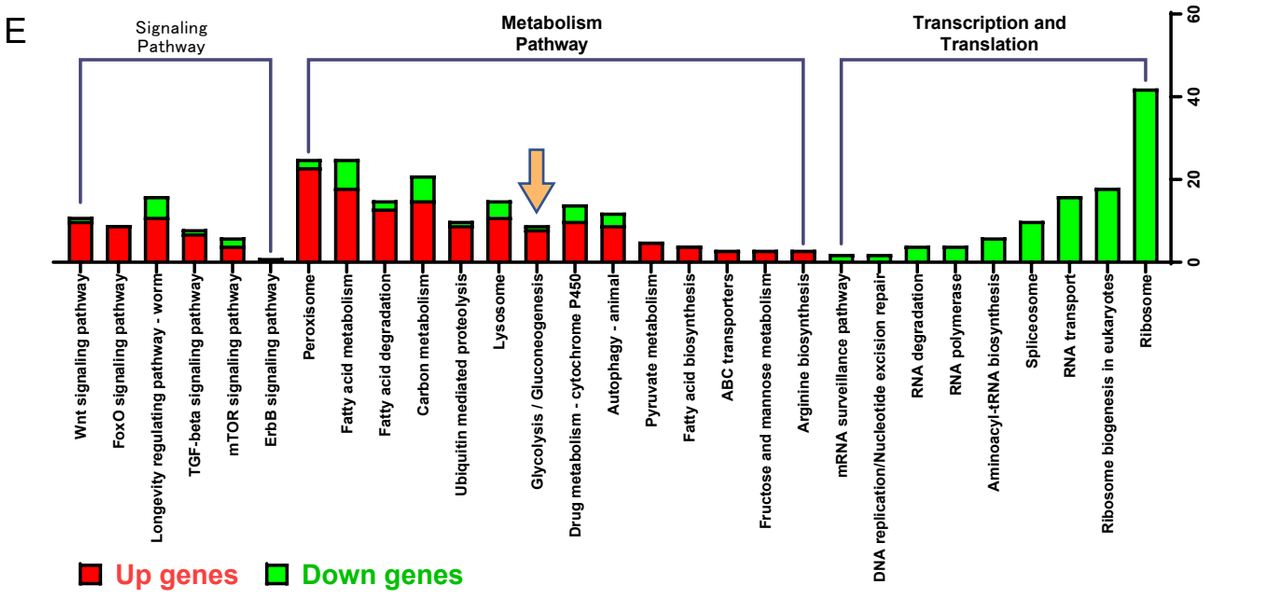
E
Signaling
Pathway
Metabolism
Pathway
Transcription and
Translation
Wnt signaling pathway
FoxO signaling pathway
Longevity regulating pathway - worm
TGF-beta signaling pathway
mTOR signaling pathway
ErbB signaling pathway
Peroxisome
Fatty acid metabolism
Fatty acid degradation
Carbon metabolism
Ubiquitin mediated proteolysis
Lysosome
Glycolysis / Gluconeogenesis
Drug metabolism - cytochrome P450
Autophagy - animal
Pyruvate metabolism
Fatty acid biosynthesis
ABC transporters
Fructose and mannose metabolism
Arginine biosynthesis
mRNA surveillance pathway
DNA replication/Nucleotide excision repair
RNA degradation
RNA polymerase
Aminoacyl-tRNA biosynthesis
Spliceosome
RNA transport
Ribosome biogenesis in eukaryotes
Ribosome
Up genes
Down genes

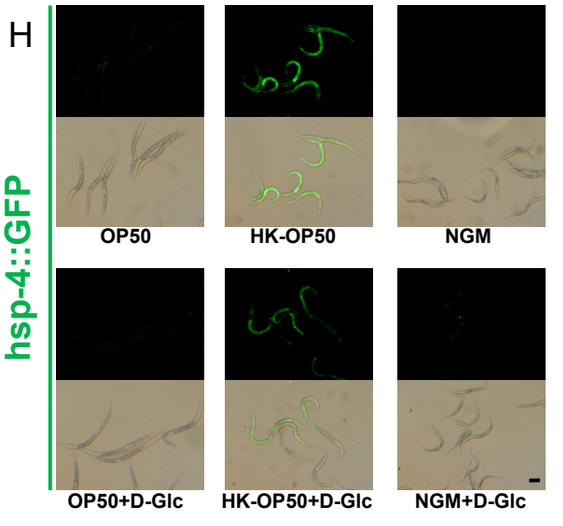
H
hsp-4::GFP
OP50
HK-OP50
NGM
OP50+D-Glc
HK-OP50+D-Glc
NGM+D-Glc

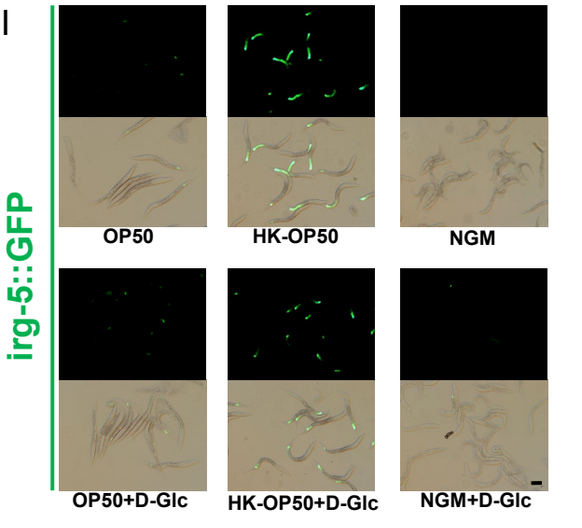
I
irg-5::GFP
OP50
HK-OP50
NGM
OP50+D-Glc
HK-OP50+D-Glc
NGM+D-Glc

Figure S3. Low sugar food, HK-*E. coli*, induce stress response and avoidance behavior in animals. Relative to Figure 3.

(A) Flow chart of strategy for *E. coli* keio mutant screening. We identified 20 *E. coli* mutants that did not induce *hsp-4::GFP* through the UPR^{ER} reporter (*irg-5::GFP*) after three rounds of screening (Table S3). From these 20 E. coli mutant, we identified 9 *E. coli* mutants that did not induce *irg-5::GFP* through the immunity reporter (*irg-5::GFP*) screening (Table S3).

(B-C) The bar graph showing that HK-*E. coli* induced *Phsp-4::GFP* (B) and *Pirg-5::GFP* (C) was decreased in animals fed mutant *E. coli* (Heat-killed). n is the number of worms scored from at least three independent experiments. Data are represented as mean ± SD.

(D) Venn diagram showing the number of deferentially metabolites in HK-*E. coli*-K12, HK-*E. coli-yfbR* and *E. coli*.

(E) KEGG enrichment analysis of deferentially expressed genes in animals fed HK-*E. coli* vs live *E. coli*. We noticed that all most of glycolysis/gluconeogenesis genes are up-regulated in animals fed HK-*E. coli*.

(F) The bar graph showing that HK-E. coli induced *Phsp-4::GFP* was not affected in animals with D-(+)-Trehalose supplementation. n is the number of worms scored from at least three independent experiments. Data are represented as mean ± SD. .

(G) GFP fluorescence images and bar graph showing that HK-*E. coli* induced *Psysm-1::GFP* was decreased in animals with D-(+)-Glucose (D-Glc) supplementation. n is the number of worms scored from at least three independent experiments. Data are represented as mean ± SD.

(H) UPR^{ER} Reporter (Phsp-4::GFP) expression animals with D-Glc supplementation under OP50, HK-OP50, or NGM condition.

(I) immunity Reporter (Pirg-5::GFP) expression animals with D-Glc supplementation under OP50, HK-OP50, or NGM condition.

For all panels, Scale bar shows on indicated figures, 50 μm. * $p<0.05$, ** $p<0.01$, *** $p < 0.001$, **** $p<0.0001$, ns: no significant difference. Precise P values are provided in Raw Data.

Figure S4

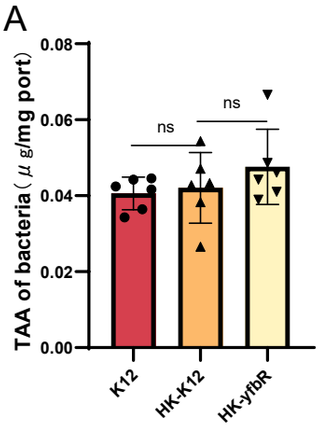
A
TAA of bacteria（μg/mg port）
0.08
0.06
0.04
0.02
0.00
ns
ns
K12
HK-K12
HK-yfbR

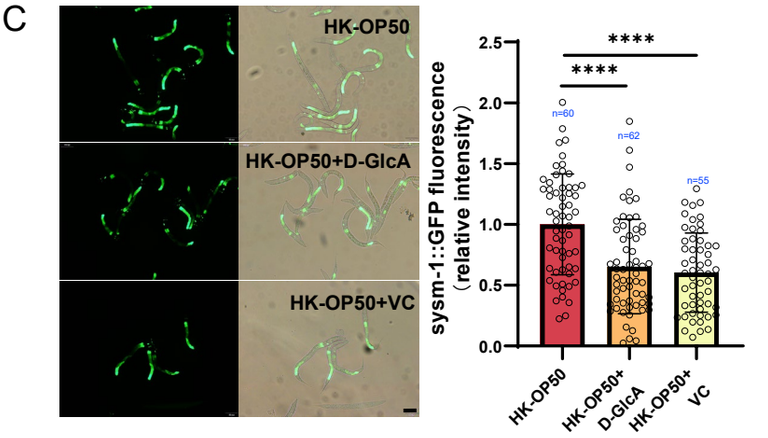
C
HK-OP50
HK-OP50+D-GlcA
HK-OP50+VC
sysm-1::GFP fluorescence
（relative intensity）
2.5
2.0
1.5
1.0
0.5
0.0
****
****
n=60
n=62
n=55
HK-OP50
HK-OP50+
D-GlcA
HK-OP50+
VC

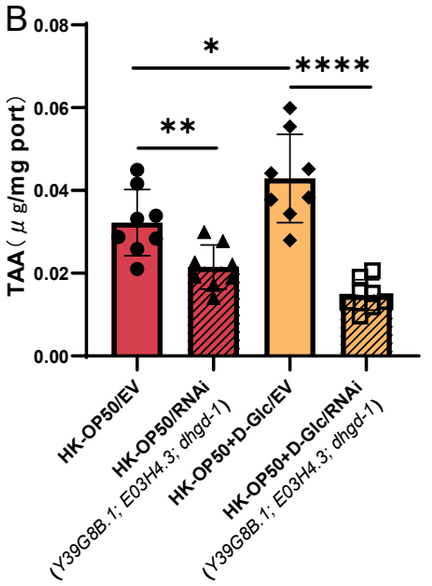
B
TAA（μg/mg port）
0.08
0.06
0.04
0.02
0.00
*
****
**
HK-OP50/EV
HK-OP50/RNAi
(Y39G8B.1; E03H4.3; dhgd-1)
HK-OP50+D-Glc/EV
HK-OP50+D-Glc/RNAi
(Y39G8B.1; E03H4.3; dhgd-1)

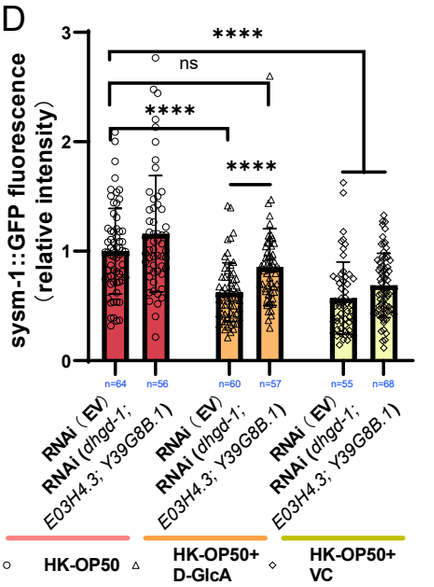
D
sysm-1::GFP fluorescence
（relative intensity）
3
2
1
0
****
ns
****
****
n=64
n=56
n=60
n=57
n=55
n=68
RNAi（EV）
RNAi (dhgd-1;
E03H4.3; Y39G8B.1)
HK-OP50
HK-OP50+
D-GlcA
HK-OP50+
VC

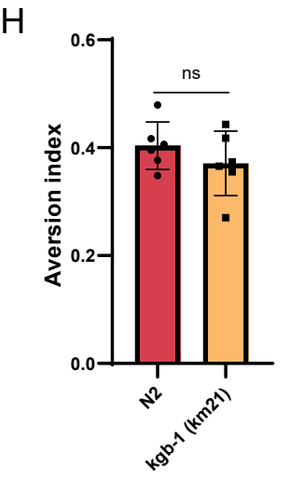
H
Aversion index
0.6
0.4
0.2
0.0
ns
N2
kgb-1 (km21)

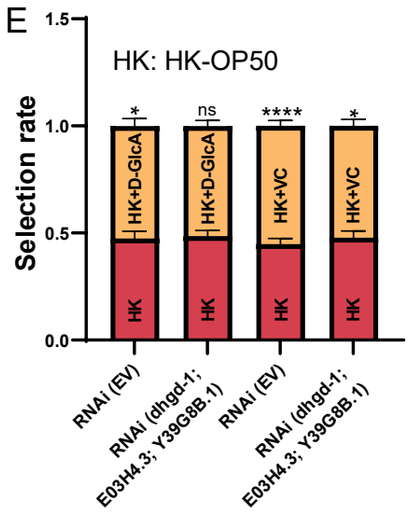
E
HK: HK-OP50
Selection rate
1.5
1.0
0.5
0.0
*
ns
****
*
HK+D-GlcA
HK+VC
HK
RNAi (EV)
RNAi (dhgd-1;
E03H4.3; Y39G8B.1)

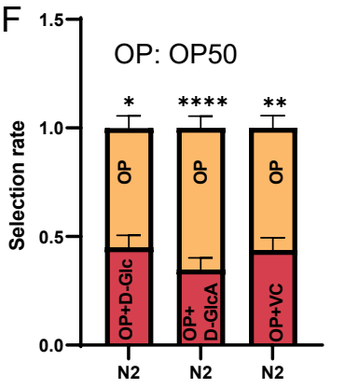
F
OP: OP50
Selection rate
1.5
1.0
0.5
0.0
*
****
**
OP
OP+D-Glc
OP+
D-GlcA
OP+VC
N2

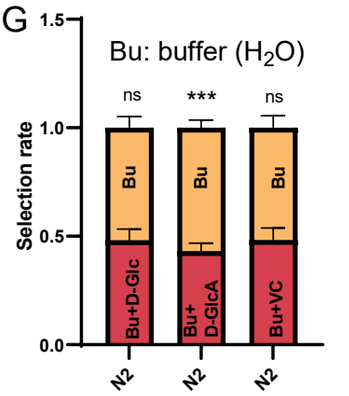
G
Bu: buffer (H2O)
Selection rate
1.5
1.0
0.5
0.0
ns
***
ns
Bu
Bu+D-Glc
Bu+
D-GlcA
Bu+VC
N2

Figure S4. Vitamin C biosynthesis pathway is critically for evaluating low sugar. Relative to Figure 4.

(A) The level of total L-ascorbic acid (TAA) in Live-K12, HK-K12, or HK-yfbR. N is number of independent experiments. Data are represented as mean ±SD from six independent experiments.

(B) The level of total L-ascorbic acid (TAA) in animals fed HK-*E. coli* with or without D-Glc supplementation. Data are represented as mean ±SD from from eight independent experiments.

(C) GFP fluorescence images and bar graph showing that HK-*E. coli* induced *Psysm-1::GFP* was decreased in animals with D-GlcA or Vitamin C supplementation. n is the number of worms scored from at least three independent experiments. Data are represented as mean ± SD.

(D) The bar graph showing that suppression of HK-*E. coli* induced *Psysm-1::GFP* by D-GlcA supplementation was abolished in animals with RNAi of VC biosynthesis genes, which was not affect by Vitamin C supplementation. n is the number of worms scored from at least three independent experiments. Data are represented as mean ±SD.

(E) Food selection assay showing that the preference of HK-*E. coli* with D-GlcA supplementation was abolished in animals by RNAi of Vitamin C biosynthesis genes. Data are represented as mean ±SD from six independent experiments, 427-775 animals/assay.

(F) Food selection assay for OP50 & OP50 + + D-Glc, D-GlcA, or VC, respectively. Data are represented as mean ±SD from five independent experiments, 241-1182 animals/assay.

(G) Food selection assay for buffer & buffer + D-Glc, D-GlcA, or VC, respectively. Data are represented as mean ±SD from five independent experiments, 8-153 animals/assay.

(H) Food avoidance assay for N2 & kgb-1 mutant animals fed with HK-E. coli. Data are represented as mean ±SD from six independent experiments, 348-660 animals/assay.

For all panels, Scale bar shows on indicated figures, 50 μm. * $p<0.05$, ** $p<0.01$, *** $p < 0.001$, **** $p<0.0001$, ns: no significant difference. Precise P values are provided in Raw Data.